doi:10.1016/j.jmb.2004.10.001 J. Mol. Biol. (2004) 344, 1311–1330

JMB

Available online at www.sciencedirect.com

SCIENCE DIRECT®

ELSEVIER

Changes in the Structure of DNA Molecules and the Amount of DNA Per Plastid During Chloroplast Development in Maize

Delene J. Oldenburg and Arnold J. Bendich*

Department of Biology
University of Washington
Seattle, WA 98195-5325, USA

We examined the DNA from chloroplasts obtained from different tissues of juvenile maize seedlings (from eight to 16 days old) and adult plants (50–58 days old). During plastid development, we found a striking progression from complex multigenomic DNA molecules to simple subgenomic molecules. The decrease in molecular size and complexity of the DNA paralleled a progressive decrease in DNA content per plastid. Most surprising, we were unable to detect DNA of any size in most chloroplasts from mature leaves, long before the onset of leaf senescence. Thus, the DNA content per plastid is not constant but varies during development from hundreds of genome copies in the proplastid to undetectable levels in the mature chloroplast. This loss of DNA from isolated, mature chloroplasts was monitored by three independent methods: staining intact chloroplasts with 4′,6-diamidino-2-phenylindole (DAPI); staining at the single-molecule level with ethidium bromide after exhaustive deproteinization of lysed chloroplasts; and blot-hybridization after standard DNA isolation procedures. We propose a mechanism for the production of multigenomic chloroplast chromosomes that begins at paired DNA replication origins on linear molecules to generate a head-to-tail linear concatemer, followed by recombination-dependent replication.

Keywords: chloroplast; DAPI; DNA replication; fluorescence microscopy; maize

*Corresponding author

Introduction

According to the standard view, the DNA within chloroplasts exists as a genome-sized circular molecule[1] that replicates by a D-loop-to-theta-to-rolling circle mechanism.[2] The DNA is associated with proteins and RNA as a nucleoid, and is inherited when nucleoids are partitioned into daughter plastids during plastid division.[3] The number of genome-sized circles per nucleoid decreases as large nucleoids in young plastids fragment and disperse throughout the expanding chloroplast,[3] presumably reaching a constant number of circles that is maintained throughout the period of maximum photosynthetic capacity of the cell. The standard view was challenged recently, when we reported that chloroplast DNA (cpDNA) molecules are highly variable in size and structure among individual chloroplasts obtained from entire shoots of maize seedlings.[4] We proposed that replication initiates through strand invasion of linear molecules to produce multigenomic branched chromosomes.

The DNA-specific fluorochrome 4′,6-diamidino-2-phenylindole (DAPI) has been used to monitor changes in the number, form, and DNA content of nucleoids during plastid development.[5–8] The size and DNA content of the nucleoids generally increase early in plastid development and then decrease as plastids divide. After cell division ceases, the number of plastids per cell increases, and the observed decrease in DNA per chloroplast was attributed to plastid division without additional cpDNA synthesis. Using various methods, including staining with DAPI, developmental changes in DNA content per plastid

Abbreviations used: DAPI, 4′,6-diamidino-2-phenylindole; cpDNA, chloroplast DNA; PFGE, pulsed-field gel electrophoresis; FI, fluorescence intensity; MS, mesophyll; BS, bundle sheath; LSC, long single copy; IR, inverted repeat; RDR, recombination-dependent replication; OPaLI, origin paired linear isomers; HSV, herpes simplex virus; h-t, head-to-tail.

E-mail address of the corresponding author: bendich@u.washington.edu

have been reported for spinach,[9] pea,[10,11] oat,[12,13] wheat,[8,14] and barley.[15] In barley, for example, the cpDNA content fell from a maximum of about 220 genome copies per plastid in the region above the basal meristem of four days old seedlings to about 50 copies per chloroplast in the leaf tip of seven to 12 days old seedlings.[15] Typically, however, only chloroplasts from young seedlings were studied, and data for mature plant tissues were not reported.

A lack of DAPI-DNA staining in chloroplasts was first reported for *Acetabularia* sp. in 1970,[16] and was presumed to be unique to the algal family, Dasycladacea.[5] The difference between chloroplasts without DNA in the vegetative stalk and with DNA in the generative cysts was attributed to differences in the rate of plastid division and unequal partitioning of nucleoids between daughter plastids.[17] A programmed loss of cpDNA in the zygote of *Chlamydomonas*[18] and the pollen of *Pelargonium zonale*[19] was associated with uniparental inheritance and was not considered to represent a more general phenomenon. In contrast, Sears & VanWinkle-Swift proposed a biochemical reason for cpDNA loss: DNA could serve as a nutrient.[20] They did not, however, extend their interpretation beyond starvation-induced gamete development in *Chlamydomonas*. The loss of DNA from chloroplasts was proposed to cause leaf senescence in coleoptiles and young leaves of rice,[21,22] but might represent recycling of DNA nucleotides as nutrients. Since the leaf tissue began to senesce two days after the loss of cpDNA, it is problematic as to whether cpDNA degradation induces senescence or reflects some general aspect of chloroplast maturation in leaves. Thus, it would be useful to examine cpDNA stability in leaf tissue that persists during the peak period of photosynthetic activity.

We recently described the demise of cpDNA during chloroplast development in *Arabidopsis*,[23] as well as the structure of cpDNA from entire shoots of young maize seedlings.[4] Here, we show that both the size and structure of individual cpDNA molecules change drastically during maize leaf development. We find that the amount of cpDNA falls to an undetectable level in mature chloroplasts from leaves that continue to conduct photosynthesis for several months. Thus, the chromosome in plastids is not constant during development, as it is in the nucleus of the cell.

Results

Maize growth and development: tissue used for analysis of chloroplasts and cpDNA

In this study, we examined plastids from young seedlings eight to 16 days old with only one or two juvenile leaves and mature plants 50–58 days old with six or seven adult leaves (Figure 1). The adult plants were in the "prime of life", presumably operating at peak photosynthetic capacity, and no reproductive organs (tassels or ears) were yet visible.

In maize and other grasses, a leaf is typically given two descriptors, the leaf number (L*n*) and the plastochron index number (P*n*), to describe its stage of development. The leaf number indicates the

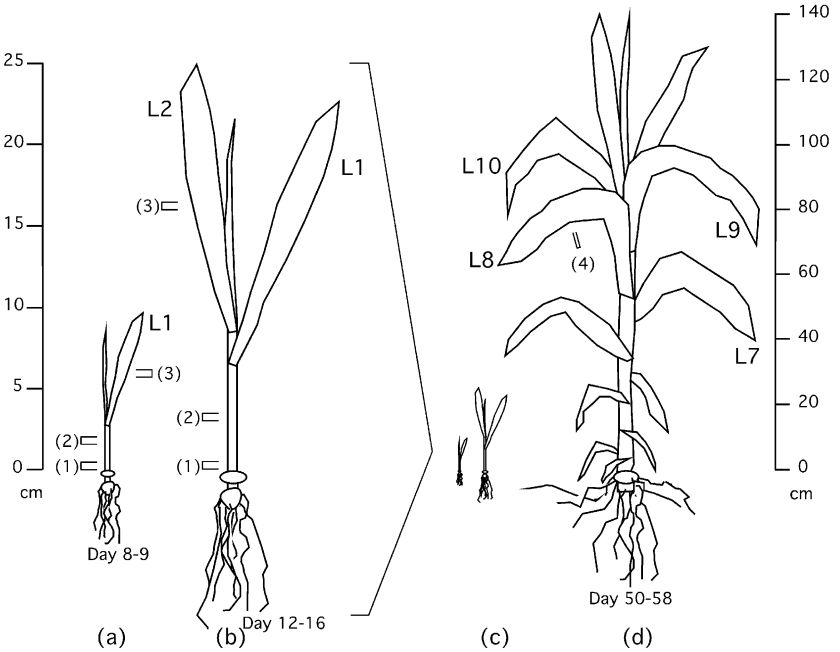

Figure 1. Maize developmental stages and tissue source of plastids. Seedlings were harvested at (a) eight to nine days or (b) 12–16 days after imbibition, and plastids were isolated from a 0.5 cm stem section that includes (1) the basal meristem directly above the node from which secondary roots will emerge, (2) the middle of the stem containing both dividing cells from the developing immature leaves and non-dividing cells from the mature L1 and L2 sheaths, and (3) the center of the mature juvenile leaf blade that would be comprised of non-dividing cells. The coleoptile was removed before harvest. Adult leaves were harvested from plants that were between 50 and 58 days old. (4) Plastids were isolated from a 1 cm section from the middle of the L8 leaf blade that would be comprised of non-dividing cells, after the midrib of the leaf blade was removed. The scale on the left applies to (a) and (b) and shows the approximate height of the seedlings at harvest. The scale on the right applies to (c) and (d) and shows the height of (c) the young seedlings and (d) the adult plant, which had not flowered. The leaf number is indicated by L1, L2, etc. The node is indicated by the oval below the stem and above the seed and roots in (a) and (b).

order in which the leaves emerge, with L1 as the first leaf after the coleoptile. The plastochron is a relative measure of time between the formation of one leaf and those that are initiated before or after it. Therefore, a newly emerging leaf would be younger, have a lower P number, and a higher L number than an older, mature leaf. In this study, we use the L number and the plant age (D) given as days after imbibitions. Our stem sections included a portion of several leaves and thus would include several plastochron numbers. On the other hand, our L number indicates tissue from the blades of individual juvenile and adult leaves.

In maize, the sheath surrounds the emerging younger leaves and forms the stem. The blade is flat and broad, and in a mature leaf extends away from the sheath at an angle. Leaves 1 (L1) through 3 (L3) are juvenile leaves, L4 and L5 are transitional leaves, and L6 and above are considered adult leaves.[24] In terms of leaf age, however, the juvenile leaves are produced first; a juvenile L2 leaf would be older than an adult L8 leaf.

For the young seedlings, we isolated and analyzed chloroplasts and cpDNA from three regions (Figure 1(a) and (b)). The base of the stem would be composed primarily of dividing cells. The middle of the stem would contain both dividing (young developing leaves) and non-dividing (sheath of mature juvenile leaves) cells. The mature leaf blade would be composed primarily of non-dividing, differentiated cells. There was a pronounced difference in the size and appearance of the plastids from these three regions of the young seedlings. Most of the plastids from the base of the stem in both the D8 and D13 seedlings were small and usually colorless, with an average size of 5 μm^2 and 7 μm^2, respectively (Figures 2 and 3; Table 1). The plastids from the middle of the stem were more variable in appearance: some were colorless, and others had dark regions with internal structure, perhaps representing the prolamellar body. These plastids were about twice the size (11 μm^2 from D8; 16 μm^2 from D13) of the proplastids in the basal meristem. In the mature L1/D8 and L2/D13 blades, the plastids were green and appeared to be fully differentiated chloroplasts with an average size of 38 μm^2 in both samples. The size range was several-fold for both tissues (Table 1).

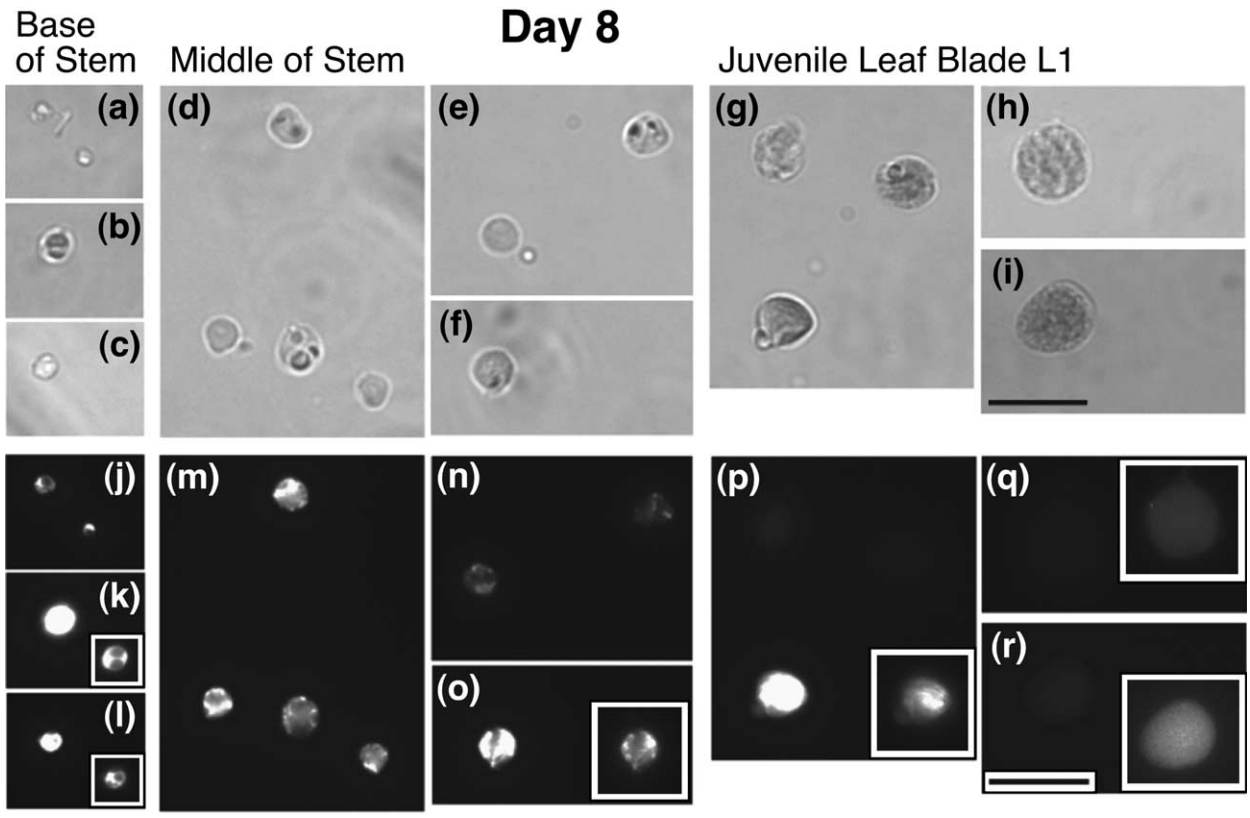

Figure 2. Plastids from eight day old juvenile seedlings imaged by bright-field microscopy and DAPI-DNA fluorescence. Representative images of plastids isolated from (a)–(c) and (j)–(l) the base, and (d)–(f) and (m)–(o) middle of the stem, and (g)–(i) and (p)–(r) L1 leaf blade from eight day old maize seedlings (see Figure 1). (a)–(i) Bright-field images. (j)–(r) DAPI-DNA fluorescence images. The fluorescence images in (j)–(r) and in (n)–(z) Figures 3 and (e)–(h) 4 are all shown at equivalent contrast enhancement levels to facilitate comparison. For the insets in (k), (l), (o), and (p), the contrast has been enhanced (decreased) to reveal the plastid nucleoids. For the insets in (q) and (r), the contrast has been enhanced (increased) to reveal the autofluorescence of the mature chloroplasts and to show that there was weak DAPI-DNA fluorescence in some mature chloroplasts ((r), for example, but not in (q)). The scale bars in (i) and (r) represent 10 μm. All images in Figures 2–4 are at the same magnification.

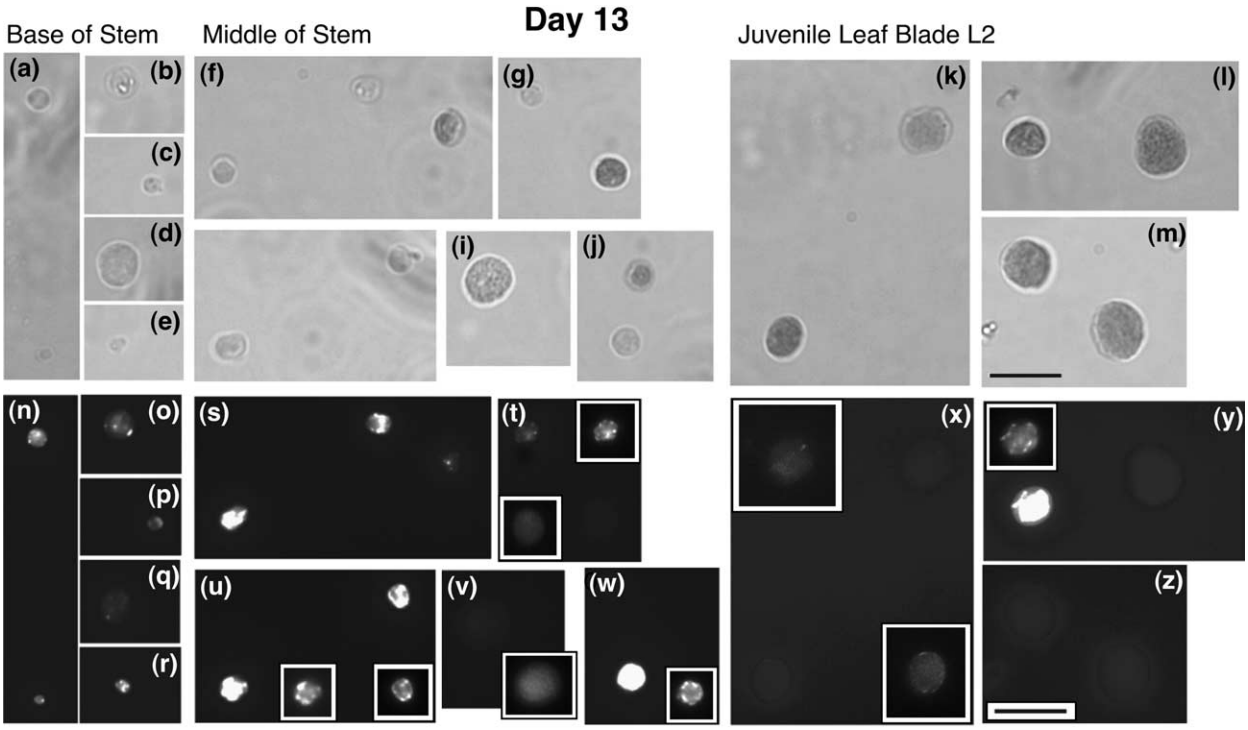

Figure 3. Plastids from 13 days old juvenile maize seedlings imaged by bright-field microscopy and DAPI-DNA fluorescence. Representative images of plastids isolated from (a)–(e) and (n)–(r) the base and (f)–(j) and (s)–(w) middle of the stem and (k)–(m) and (x)–(z) L2 leaf blade (see Figure 1). (a)–(m) Bright-field images. (n)–(z) DAPI-DNA fluorescence images. For the insets in (u), (w), and (y), the image contrast has been enhanced (decreased). For the insets in (t), (v) and (x), the image contrast has been enhanced (increased). The scale bars in (m) and (z) represent 10 μm.

Table 1. Size and DAPI fluorescence of maize plastids

Tissues[a]	Area[b]	DAPI FI/ plastid[c]	Total DAPI F/plastid[d]	CorTotal DAPI F/plastid[e]	Number of plastids[f]	Number DAPI F=0 [g]	% Plastids DAPI F=0
Day 8							
Base of stem	5±2 (1–11)	641±247 (93–1108)	2848±1769 (476–6752)	2718 (397–6095)	20	0	0
Middle of stem	11±4 (3–23)	429±150 (71–811)	4405±2183 (444–9447)	3695 (0–8256)	43	1	2
L1 juvenile leaf	38±12 (25–64)	168±154 (81–567)	5258±3770 (2242–14829)	1751 (0–12341)	15	8	53
Day 13							
Base of stem	7±5 (2–35)	154±73 (21–305)	868±580 (79–2727)	585 (0–1653)	66	5	5
Middle of stem	16±6 (7–37)	180±143 (6–532)	2585±2155 (109–9263)	1585 (0–1047)	55	21	38
L2 juvenile leaf	38±14 (12–73)	61±62 (15–318)	2058±2130 (212–11549)	467 (0–9210)	50	44	88
Day 58							
L8 adult leaf	33±11 (12–72)	90±38 (31–265)	2444±1934 (278–14271)	212 (0–7019)	112	97	89

Note that the Total DAPI F in L1, L2, and L8 is much larger than the CorTotal DAPI F because the Total DAPI F in the green chloroplast is almost entirely due to autofluorescence, not DAPI-DNA fluorescence. The high standard deviations are due to the wide range among individual plastids and thus may not be significant. The value for CorTotal DAPI F/plastid is zero for some plastids; thus the standard deviation is not presented.

[a] The tissues from which the plastids were isolated correspond to those indicated in Figure 1.

[b] Plastid area (μm^2) was measured under white light. The mean area±standard deviation (range among plastids) is given.

[c] The fluorescence intensity (FI) of DAPI-DNA stained plastids was determined (Materials and Methods). The mean FI±standard deviation (range among plastids) is given. The FI units are in pixels. The DAPI FI/plastid has been corrected for slide-to-slide variation in the background DAPI fluorescence, but not for plastid autofluorescence (see Materials and Methods).

[d] The area of DAPI fluorescence (not the white light area) multiplied by the DAPI FI. Total DAPI F units are pixel·μm^2.

[e] Total DAPI F corrected for plastid autofluorescence, as described in Materials and Methods. Note that except for D8 base of stem, the lowest value in the range is given as zero. Zero indicates that if there was any DNA in the plastid, it was undetectable. The lowest value above zero was 372 for D8 middle of stem, 32 for D8/L1, 23 for D13 base of stem, 98 for D13 middle of stem, 1857 for D13/L2, and 14 for D58/L8.

[f] The number of plastids measured.

[g] The number of plastids with no detectable DAPI-DNA fluorescence, after adjusting for plastid autofluorescence.

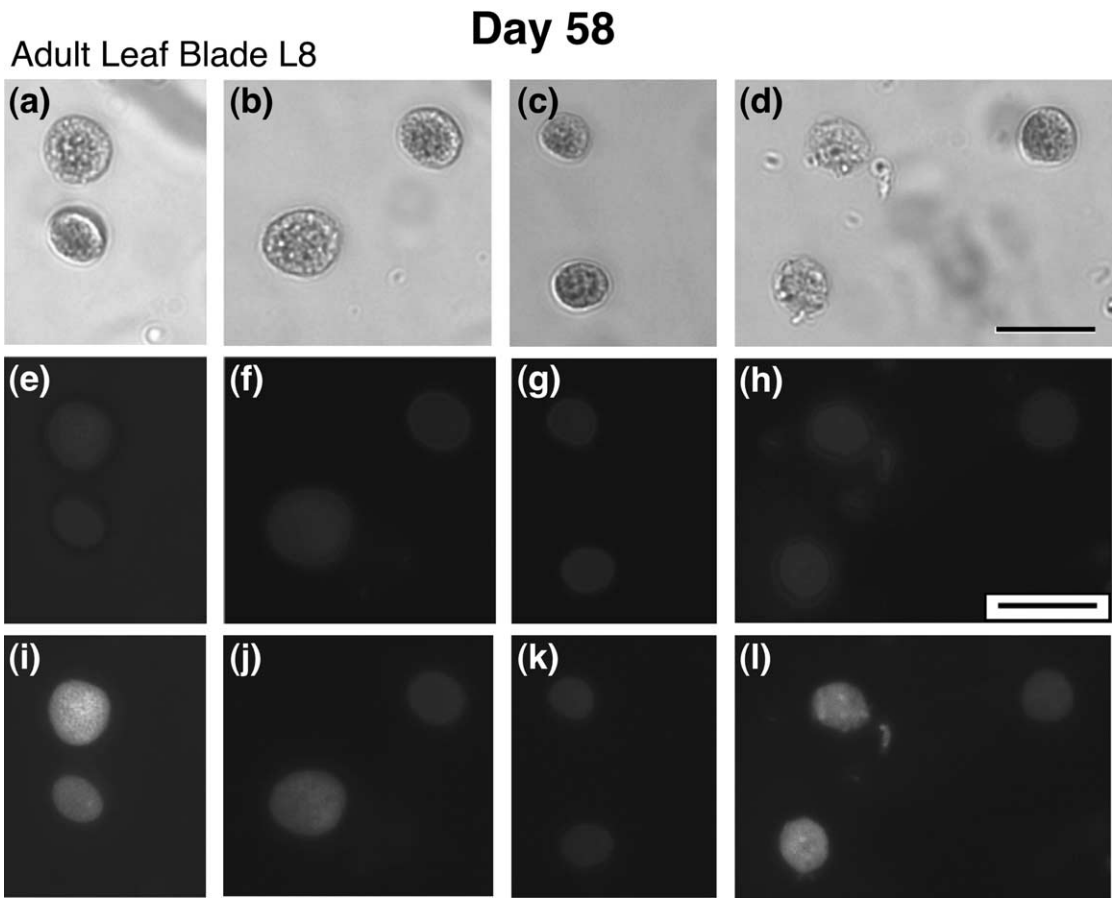

Figure 4. Plastids from 58 days old adult plants imaged by bright-field microscopy and DAPI-DNA fluorescence. Representative images of plastids isolated from the L8 adult leaf blade (see Figure 1). (a)–(d) Bright-field images. (e)–(h) DAPI-DNA fluorescence images. (i)–(j) The same images shown in (e)–(h), except the contrast has been enhanced (increased). The scale bars in (d) and (h) represent 10 μm.

For the adult plants, we isolated and analyzed chloroplasts and cpDNA only from the blade of leaves L7–L10 which are mature, adult leaves. In this case, the cells would be fully differentiated and should be operating at peak photosynthetic capacity. The plastids from the mature leaf blade (L8/D58) appeared to be fully developed chloroplasts, green in color under white light with an average size of 33 μm^2 (Figure 4 and Table 1). As found for D8 and D13 tissues, these chloroplasts varied greatly in size (12–72 μm^2; Figure 5).

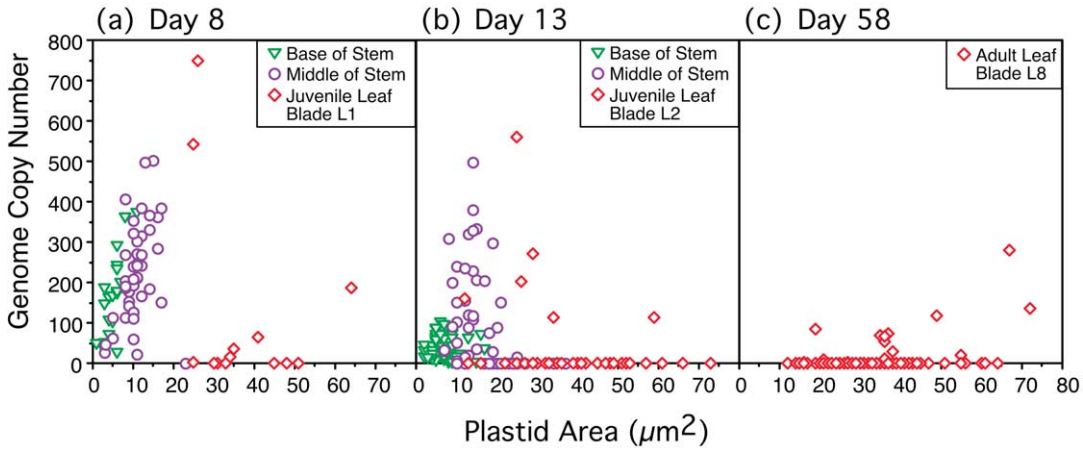

Figure 5. Genome copy per plastid and plastid area for juvenile and adult plants. Data are given for tissues from the basal meristem (triangles), middle of the stem (circles), and leaf blade (diamonds) from (a) eight days old, and (b) 13 days old juvenile seedlings and (c) a 58 days old adult plant (see Figure 1). Each point represents one plastid.

Nucleoid DAPI fluorescence and DNA content in maize chloroplasts

Plastids were isolated and stained with DAPI to visualize the DNA in the nucleoids (Figures 2–4). The isolated organelles were plastids for three reasons. (1) Our preparative method is known to yield plastids and exclude nuclei and mitochondria. (2) The changes during leaf development (described above and below) are characteristic of plastids (not nuclei or mitochondria) and include green coloration, organelle size, and the number, size and distribution of nucleoids. (3) The DNA obtained from the organelles is shown below to be cpDNA by blot-hybridization and mobility during pulsed-field gel electrophoresis (PFGE).

The DAPI fluorescence intensity (FI) was used to determine the DNA content per plastid (Figures 5 and 6; Tables 1 and 2). The genome copy number per plastid was calculated from the total DAPI fluorescence per plastid (FI multiplied by the plastid area) and the DAPI fluorescence from particles of either vaccinia virus or bacteriophage T4 used as DNA standards. We found an approximately twofold difference in the plastid genome copy number, depending on whether vaccinia virus or T4 was used as the standard (Table 2). The degree of DNA compaction may influence DAPI-DNA FI[25] and have contributed to this twofold difference. The genome copy numbers reported below and shown in Figures 5 and 6 were calculated using the vaccinia virus genome standard (see Materials and Methods), because the fluorescence was weaker with a higher background using T4, and essentially all of the DNA from our vaccinia virus particles migrated as a single band during PFGE (we did not examine T4 by PFGE).[26]

For most proplastids at the base of the stem, there was a single nucleoid with bright DAPI-DNA fluorescence, seen either as a partial ring around the plastid or as spots joined by a thinner strand (Figure 2). Other plastids contained one or more bright spots, usually at the periphery, with fainter fluorescence throughout the plastid. In the plastids from the middle of the stem of the D8 and D13 seedlings, the nucleoids were variable in size and intensity. Frequently there were five to ten discrete spots of fluorescence, sometimes with strands connecting the spots. In a few plastids, the spots were almost continuous around the periphery of the plastid, forming a ring. In addition to the spots, there was usually a diffuse fluorescence throughout

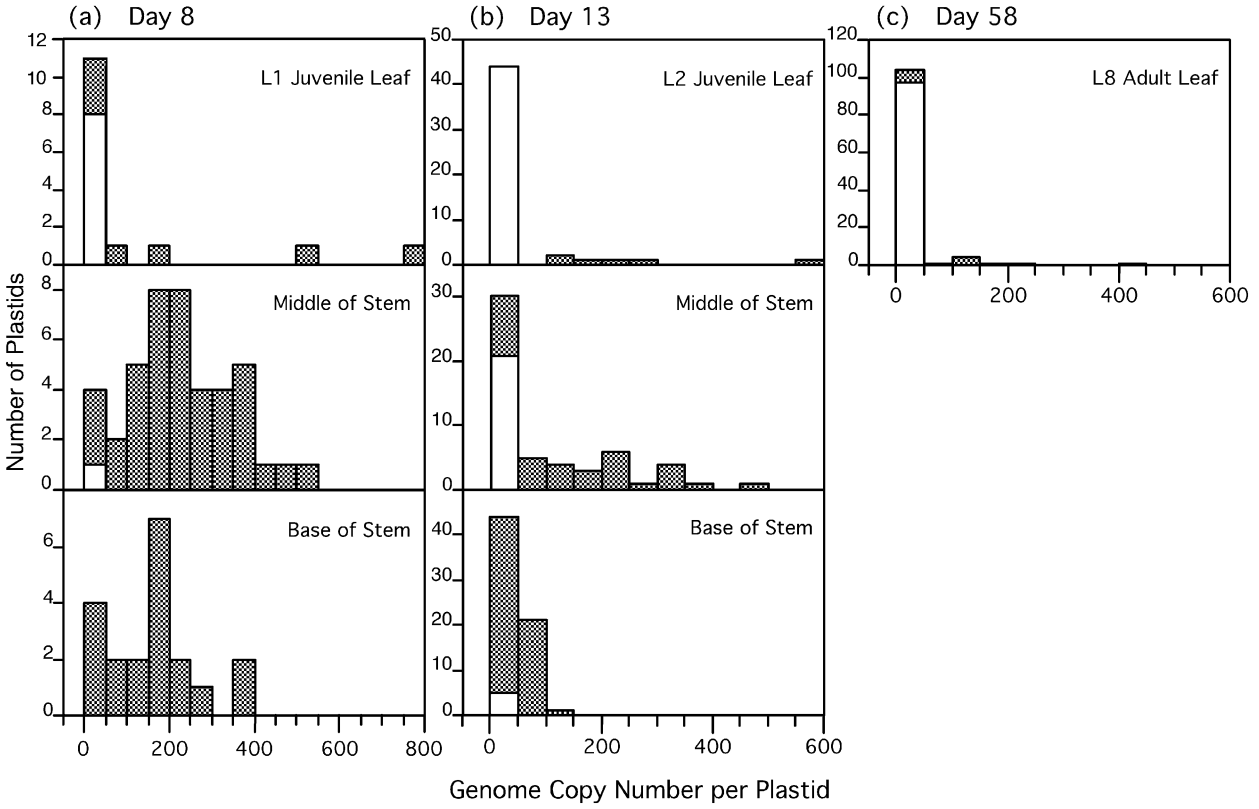

Figure 6. Genome copy number per plastid for different tissues. Plastids isolated from tissues (Figure 1) from (a) eight days old, (b) 13 days old and (c) 58 days old plants. Genome copy numbers were determined from DAPI-DNA fluorescence using the vaccinia virus genome as a standard and are grouped in 50 copy number increments. Crosshatched bars represent plastids with measurable DNA, and open bars indicate plastids with no detectable DNA. For example, the left bar in (b) Middle of stem indicates that the 0–50 interval contains 21 plastids without detectable DNA and nine plastids with DNA equivalent to between 1 and 50 copies of the 140 kb genome. Further statistical information is given in Table 2.

Table 2. Maize plastid genome copy number relative to vaccinia virus and T4 bacteriophage genomes

	Vaccinia virus						T4 bacteriophage		
	V units[b]			Copy number from V[c]			Copy number from T[d]		
Tissue[a]	Mean	Median	Range	Mean	Median	Range	Mean	Median	Range
Day 8									
Base of stem	109	110	16–244	165	168	24–371	348	353	51–780
Middle of stem	148	139	0–330	225	211	0–502	473	444	0–1057
L1 juvenile leaf	70	0	0–494	106	0	0–750	224	0	0–1580
Day 13									
Base of stem	23	20	0–66	36	30	0–100	75	63	0–212
Middle of stem	63	21	0–327	96	32	0–497	203	68	0–1047
L2 juvenile leaf	19	0	0–368	28	0	0–560	60	0	0–1179
Day 58									
L8 adult leaf	8	0	0–281	13	0	0–427	27	0	0–898

The values listed here were determined from the individual plastids plotted in Figure 5. A genome copy number of zero indicates a plastid with undetectable DAPI-DNA fluorescence after subtracting non-DAPI auto-fluorescence (Table 1). Standard deviations are not included and probably not significant because they were very high due to the wide range, and many plastids had copy numbers of zero. For example, there were only six out of 50 plastids with copy number ≥ 1 in the L2 juvenile leaf.

[a] The tissues from which the plastids were isolated correspond to those diagrammed in Figure 1.

[b] The mean, median, and range of V units per plastid is given. A V unit is the ratio of plastid CorTotal DAPI F to the total DAPI F of a vaccinia virus particle (Materials and Methods). The Total DAPI F of a vaccinia virus particle was determined as 25 ± 11 pixel$\cdot\mu m^2$, based on measuring 151 particles.

[c] Genome copy number per plastid as calculated from the V units. Note that except for D8 base of stem, the lowest copy number value given in the range is zero (undetectable CorTotal DAPI F; see Table 1). The lowest value above zero, however, was 23 for D8 middle of stem, 2 for D8/L1, 1 for D13 base of stem, 6 for D13 middle of stem, 113 for D13/L2, and 1 for D58/L8. A value of 16 ± 8 pixel$\cdot\mu m^2$ for the CorTotal DAPI F is equivalent to one plastid genome copy (see Table 1). The copy number per plastid was rounded to the nearest whole number.

[d] Copy number based on T4 bacteriophage, as for vaccinia virus (Materials and Methods). The Total DAPI F of a T4 phage particle was determined as 10 ± 6 pixel$\cdot\mu m^2$, based on measuring 150 particles.

the plastid. We would except to detect a nucleoid containing at least 42 kb, the genome size of bacteriophage P22,[27] because a P22 particle was easily detectable as a spot of DAPI-DNA fluorescence.

The fluorescence characteristics for the fully developed chloroplasts from the leaf blade were similar for the young juvenile leaves, L1/D8 and L2/D13, and the adult leaf L8/D58. Most of these mature plastids had no visible nucleoids, nor any blue-white fluorescence at all that might represent DNA. These chloroplasts did, however, have a faint reddish tinge using the DAPI filter that we attribute to plastid autofluorescence, probably from chlorophyll. In order to account for this autofluorescence, plastids were examined both with and without DAPI and with and without DNase. Both methods gave similar results: a faint reddish autofluorescence was quantified and used in calculating the DNA content (see Materials and Methods). In Figures 5 and 6, a genome copy number value of zero is given for any plastid with no detectable DAPI fluorescence (after subtracting the plastid autofluorescence). This does not imply that there is absolutely no DNA within the plastid, only that if there was any DNA it is below the level of detection in our quantitative assay. The theoretical limit of detection is 1 pixel$\cdot\mu m^2$ (above the background DAPI autofluorescence) for the CorTotal DAPI F per plastid (Table 1) and is equivalent to 9 kb of DNA (see Materials and Methods).

In both D8 and D13 seedlings, we observed a similar change in genome copy number per plastid, depending on the developmental stage of the tissue (Figure 6). The average genome copy number increased in the developing plastids in the middle of the stem compared to the copy number in the proplastids at the base of the stem (Table 2). There was a dramatic decrease in the copy number per plastid in the fully developed chloroplast from the L1/D8 and L2/D13 juvenile leaf blades compared to the plastids in the stem. The average copy number decreased further for the adult L8/D58 leaf blade.

Although the general trend in copy number per plastid with plastid development was similar between D8 and D13 seedlings, there was a difference in the copy number among similar developmental regions. For example, the average copy number at the base was 165 at D8, but was only 36 at D13 (Table 2). Although the plastids are from similar regions (base or middle of stem and leaf blade), there may nonetheless be some difference in the proportion of cells (and thus chloroplasts) at a specific developmental stage. For instance, in the D8 seedling, cell division may have ceased in the mature first leaf sheath (L1) but would still be high in the developing leaves that are enclosed by the sheath. In contrast, cell division in the D13 seedling, both L1 and L2 sheaths, may have stopped and only the developing leaves enclosed by these sheaths were still dividing. Therefore, there would be a higher proportion of dividing to non-dividing cells and undeveloped plastids in the stems of the D8 seedlings than in D13. In summary, the difference in copy number may merely reflect

the difference in overall plant development, with older plants having a higher percentage of differentiated cells and fully developed chloroplasts compared to younger plants. In support of this idea is the finding that there are more plastids with undetectable cpDNA in the stem of the D13 seedling than in D8. One out of 43 plastids in the middle of the stem from the D8 seedling had no detectable cpDNA, whereas 21 out of 55 plastids from the D13 seedling were in this "no-DNA" category (Figure 6; Table 1).

At the base of the stem in the D8 seedling, the copy number ranged from 24 to 371 genomes per plastid (Figures 5 and 6, Table 2). In the equivalent basal region of the D13 seedling, the maximum copy number was only 100, and five out of 66 plastids had no measurable cpDNA. The plastids from the center of the stem showed the greatest variability in DNA content, in both the D8 and D13 seedlings. This variability probably reflects the mixed cell populations comprised of both dividing cells in the young developing leaves and the non-dividing cells in the differentiated sheath tissue of the mature L1/D8 and L2/D13 juvenile leaves. In both the D8 and D13 seedlings, plastids with up to about 500 copies per plastid were observed. In general, the plastids from D8 had a higher copy number than those from the D13 seedling. The D13 seedling had 38% of the plastids with no measurable cpDNA, whereas only 2% of the plastids from D8 were in this category (Figure 6; Table 1), suggesting a higher percentage of differentiated cells with more fully developed plastids in the stem at D13. In the mature leaf blades, there were only a few plastids with copy number greater than 100, and about 90% of the plastids had no detectable cpDNA. The youngest leaf (L1/D8) had a higher percentage of plastids with measurable cpDNA than either L2/D13 or L8/L58, suggesting that many of its plastids have not yet fully differentiated into mature chloroplasts.

One possible explanation for the observed decline in DNA from maturing chloroplasts is that the chloroplast envelope becomes more permeable to exogenously added materials as the chloroplast develops. Thus, the DNase used in our chloroplast preparation procedure might preferentially enter mature chloroplasts and digest their DNA. To test this possibility, we examined the DAPI-DNA fluorescence of chloroplasts prepared from mature leaf tissue with and without DNase treatment (see Materials and Methods). The fraction of chloroplasts without detectable DAPI-DNA fluorescence was 85% when DNase was included and 82% when DNase was omitted, a result inconsistent with the differential permeability explanation for the decline in DNA content of mature chloroplasts. An analogous decline in *Arabidopsis* cpDNA content was similarly found not to be attributable to differential permeability.[23]

To summarize, after an increase, the DNA content per plastid decreased as the leaf tissue developed. The smaller undifferentiated plastids ($<20\ \mu m^2$) generally had more cpDNA than the larger developed chloroplast ($>20\ \mu m^2$) (Figure 5). Among the smaller plastids, there was a large variability in copy number, but there was no correlation between copy number and plastid area. In the adult leaf (L8/D58), however, there was no detectable DNA even in most of the smaller plastids. It seems that the loss of cpDNA in maize follows a developmental program.

Fluorescence microscopy of ethidium bromide-stained DNA molecules from maize chloroplasts

We previously reported cpDNA in both simple forms and complex multigenomic structures from entire shoots of 10–14 days old maize seedlings.[4] For this study, we sampled meristematic tissues, where cpDNA replication occurs, and differentiated leaves where cpDNA replication has ceased. We examined the structure of the deproteinized cpDNA from different tissues at a single plant age and from the leaf blade of both juvenile and adult plants. The cpDNA from a single microscopic field of view (which represents the DNA from a single plastid) was placed into one of three classes, according to the structure of the molecules (Figure 7(a)–(c)). The DNA in class I (Figure 7(a)) appeared as complex structures with a dense, bright core of fluorescence and several connected fibers (Figure 8(a), for example). In class II (Figure 7(b)), a bright core with or without connected fibers was observed; when present the fibers were typically shorter, and there were many more unconnected fibers of DNA (Figure 7(e)) than in class I (Figure 7(d)). For inclusion in class II, the number of unconnected fibers within a field must be greater than the number of fibers connected to the core (Figure 9(e), for example). Class II cpDNA was not observed at developmental stages 1 or 2. No fluorescent core of DNA was present in class III. Instead, a collection of unconnected fibers was seen, in some cases filling or extending beyond the field of view. In some class III fields there was a central cluster of overlapping molecules (Figure 9(g)), and in a few instances there appeared to be branching or interconnections between the molecules. The cpDNA molecules from meristematic regions (stage 1) were primarily complex forms in class I, whereas cpDNA from differentiated regions (stages 3–6) was found in the structurally simple forms of class III.

Figure 7(a) shows that for the youngest seedlings examined, D9, most of the cpDNA from both stage 1 (87%; the base of the stem) and stage 2 (75%; the middle of the stem) was in class I (Figure 8(a)–(f)). There were, however, some differences in the cpDNA structures from these two stages. The connected fibers were shorter in the class I forms from stage 2 (Figure 8(e) and (f)) than in those from stage 1 (Figure 8(a) and (b)). In addition, there was a higher percentage of fields with class III molecules (Figure 8(g)) in the middle of the stem (25%; stage 2) than at the base (13%; stage 1) (Figure 7(c)). In stage 3 (L1 leaf blade), the class I structures (29%;

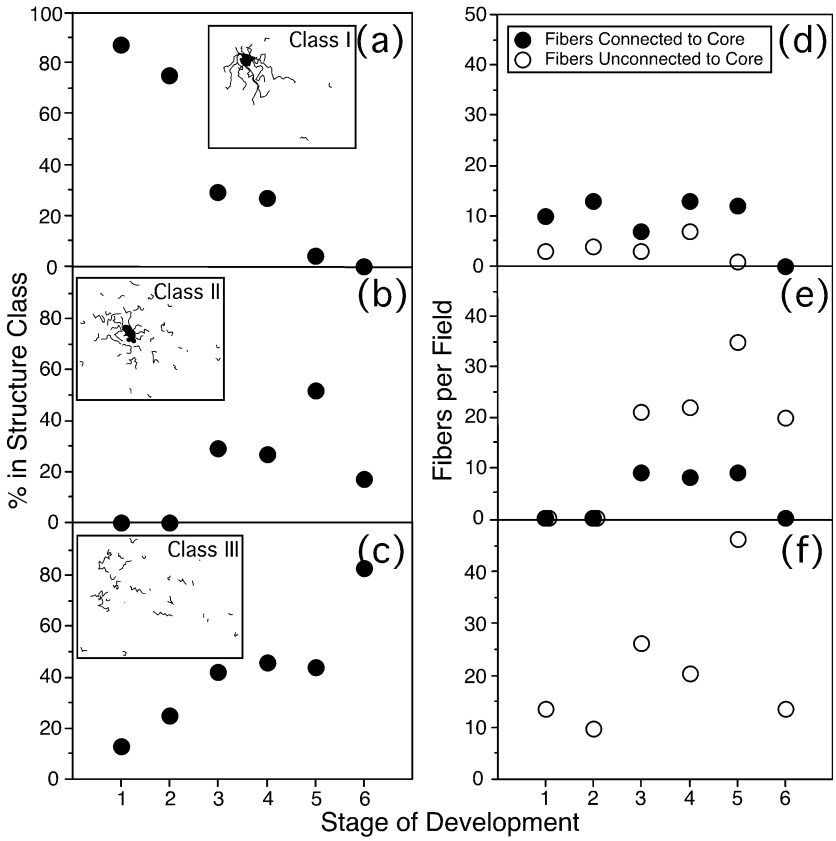

Figure 7. Classification of plastid DNA structure for different tissues. Ethidium bromide-stained plastid DNA from various stages of development was visualized by fluorescence microscopy and characterized by (a)–(c) structural class and (d)–(f) the average number of DNA fibers per field of view. (a) Class I is characterized by a single complex structure, a dense core of fluorescence with connected fibers (filled circles in (d)), and a few unconnected fibers (open circles in (d)). (b) Class II is characterized by a greater number of unconnected fibers (open circles in (e)) than fibers connected to a core (filled circles in (e)). (c) Class III is comprised exclusively of unconnected fibers (open circles in (f)). Stage 1 is the base of the stem from nine days old seedlings. Stage 2 is the middle of stem from nine days old seedlings. Stage 3 is the L1 juvenile leaf blade from nine days old seedlings. Stage 4 is the L2 juvenile leaf blade from 12 days old seedlings. Stage 5 is the L2 juvenile leaf blade from 16 days old seedlings. Stage 6 is the L7-10 adult leaf blades from 50 and 57 days old plants. In (a)–(c), the number of fields analyzed for stages 1–6, respectively, was 23, 16, 14, 11, 23, and 6. For stage 1, the range of numbers of fibers connected to a core was (d) 6–16 for class I and (e) none for class II. The corresponding values were 8–16 and none for stage 2; 4–10 and 5–15 for stage 3; 10–15 and 4–11 for stage 4; 12 and 6–17 for stage 5; none and none for stage 6. For stage 1, the range of numbers of fibers unconnected to core was (d) 0–11 for class I, (e) none for class II, and (f) 5–21 for class III. The corresponding values were 0–10, none, and 8–12 for stage 2; 3, 16–24, and 8–48 for stage 3; 6 or 7, 19–28, and 5–43 for stage 4; 1, 15–100, and 23–84 for stage 5; none, 20 and 1–22 for stage 6.

Figures 7(a) and 8(h)) decreased, and there was a corresponding increase in both class II (29%; Figures 7(b) and 8(i)) and class III (42%; Figures 7(c) and 8(j)) structures. These results suggest that the complex forms in class I represent the structure of replicating cpDNA and that after replication has ceased, there is a conversion of highly branched structures to simpler class III forms. The complex forms in Figure 8(c) and (d) have two cores (arrows 1 and 2) connected by several fibers (long arrow). Such structures may represent the cpDNA from a nucleoid undergoing division, since they are from the basal meristematic region. To summarize, the developmental progression from proplastids (at the base of the stem) to mature chloroplasts (in the expanding leaf) is accompanied by a progression from a single complex DNA structure to multiple, unconnected, small molecules (most of which appear to be much smaller than 140 kb, the size of the genome).

In addition to a change in cpDNA structure from the base of the stem to the blade of the leaf, a change in structure depending on the age of the leaf was observed (stages 3–6 in Figure 7). There was little change in cpDNA structure in the leaf blades of juvenile plants between stages 3 (L1/D9) and 4 (L2/D12) of development. Stages 3 and 4 had similar percentages of cpDNA in each structural class: 27–29% class I, 27–29% class II, and 42–46% class III (Figures 7(a)–(c); 8(h) and (i)); and 9(a)–(c)). Four days later, however, in the stage 5 leaf (L2/D16) the class I cpDNA structures decreased to 4% and the class II structures increased to 52% (Figures 7(a) and (b); and 9(d) and (e)). In class II fields of L2 (Figure 7(e)), there were also more unconnected fibers on average at D16 (stage 5; 35) than at D12 (stage 4; 22). Between D12 and D16 there was no change in the percentage of fields in class III (46% and 44%, respectively, Figure 7(c)), but there was a 2.3-fold increase in the average number of individual fibers per field (Figures 7(f); and 8(f)–(i)). For the adult plant leaves (stage 6), there was no class I structure and only one field in class II (Figure 7(a) and (b)). Most of the cpDNA (83%) was in class III (simple unconnected molecules; Figure 9(j)–(l)), but the number per field (14 fibers) was much lower than in the juvenile stage 5 leaf (48 fibers) (Figure 7(f)). For stages 1–4, almost every field per microscope slide contained ethidium bromide (EtBr)-stained cpDNA (see Materials and Methods). No DNA was found, however, in many fields from stage 5 and especially stage 6, where only five fields with cpDNA were found on an entire slide. This lack of EtBr-stained DNA in most

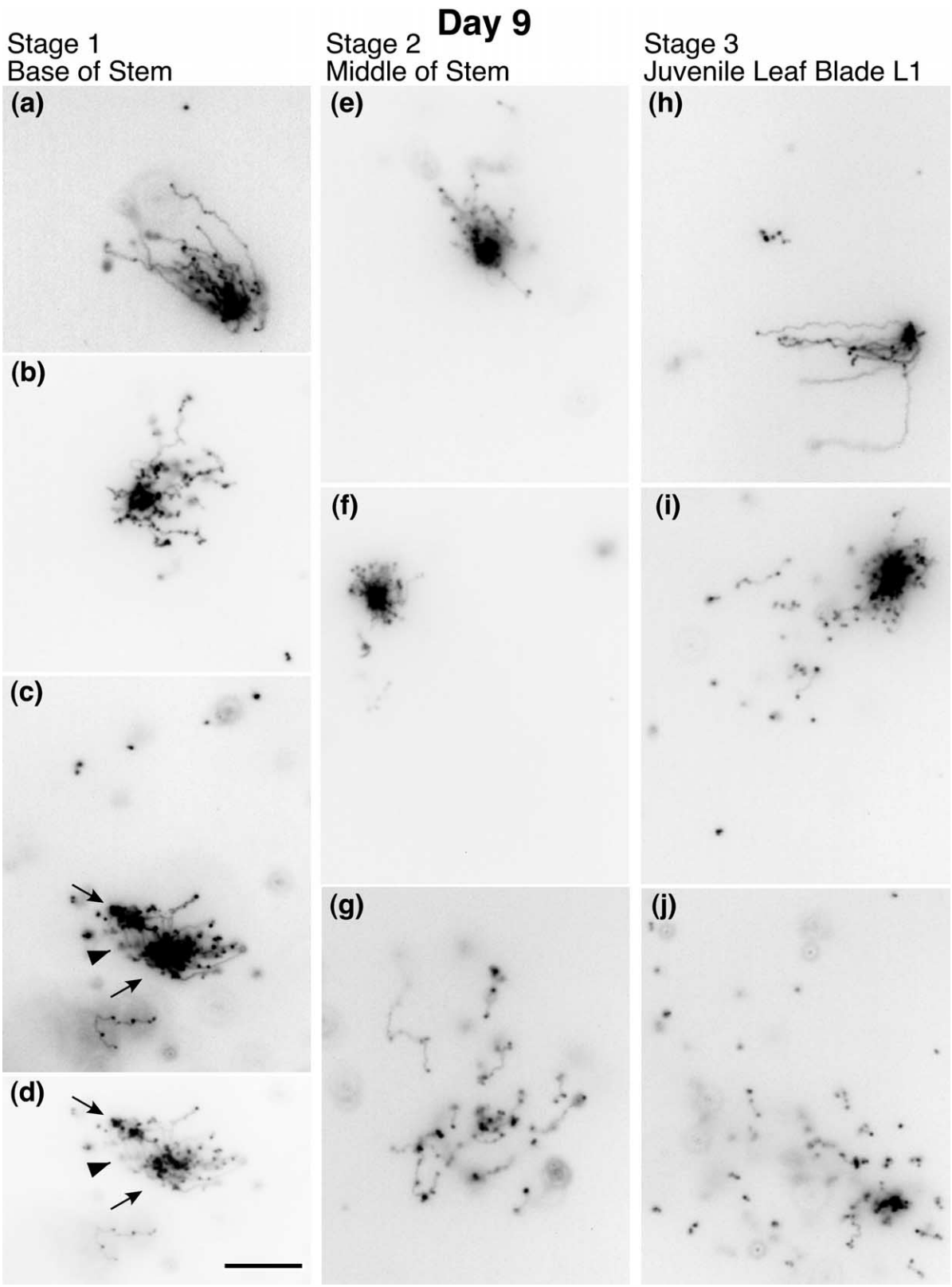

Figure 8. Total EtBr-DNA from individual plastids of nine days old juvenile seedlings. Each image shows the EtBr-DNA from a single plastid, although some unconnected fibers are not included in some images. Stages and structure classes correspond to those described in Figure 7. (a)–(c) Representative class I fields from stage 1. (d) Part of the image shown in (c), except the contrast has been enhanced (decreased). The two arrows in (c) and (d) indicate two DNA cores connected by fibers (arrowhead). This structure may represent the DNA of a dividing nucleoid. (e) and (f) Representative class I fields from stage 2. The connected fibers are shorter than in the class I fields of stage 1. (g) A representative class III field from stage 2. (h)–(j) Representative (h) class I, (i) class II and (j) class III fields from stage 3. The scale bar represents 10 μm and applies to all images.

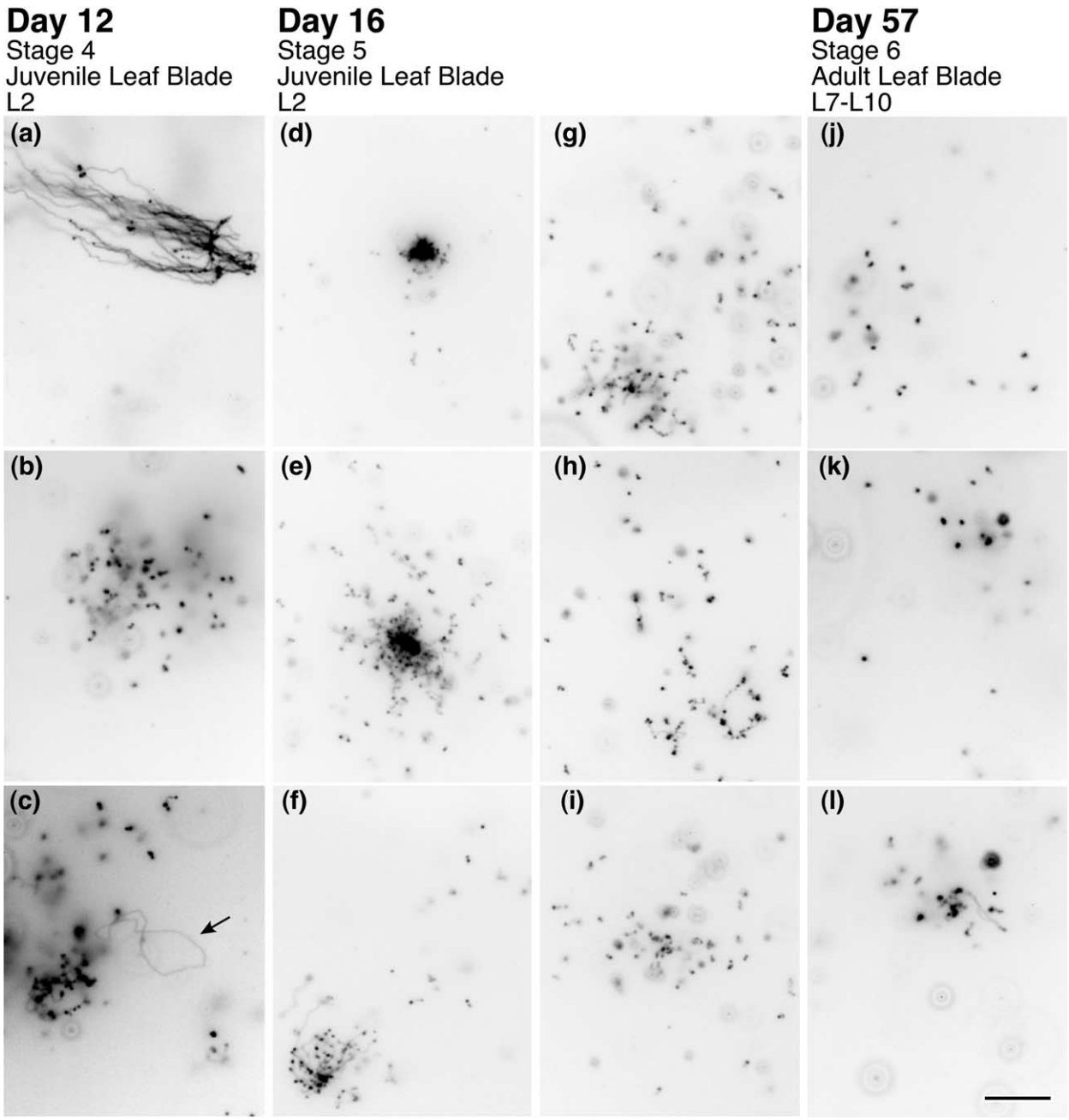

Figure 9. Total EtBr-DNA from individual plastids of juvenile and adult tissue. Each image shows the EtBr-DNA from a single plastid, although some unconnected fibers are not included in some images. Stages and structure classes correspond to those described in Figure 7. (a)–(c) Representative (a) class I and (b) and (c) class III fields from stage 4. The arrow in (c) points to a genome-sized circle. This is the only circular form found among the 93 fields analyzed for all six stages of development. (d) A representative class I field from stage 5. (e) A representative class II field from stage 5. (f)–(i) Representative class III fields from stage 5. (j)–(l) Representative class III fields from stage 6. The scale bar represents 10 μm and applies to all images.

of the fields of view indicates that most of the chloroplasts from the mature juvenile and adult leaf blades did not contain any DNA, in agreement with the results from DAPI-DNA staining (Figure 6). A similar result was obtained when we used PFGE and blot-hybridization to analyze DNA from chloroplasts (Figure 10). No cpDNA was detected from stage 6 chloroplasts in the well-bound fraction with only a faint smear of ∼50-kb DNA in the electrophoretically mobile fraction, but cpDNA was detected readily in both fractions (including mobile molecules equal to and larger than the 140 kb genome) from chloroplasts representing stages 1 and 4. Thus, the DNA detected by DAPI staining in 11% of the stage 6 mature chloroplasts (Figure 5(c)) probably represents subgenomic fragments not yet degraded completely.

The number of fibers connected to a core was similar (10 ± 5) for class I (Figure 7(d)) and class II (Figure 7(e)), but the length of these fibers

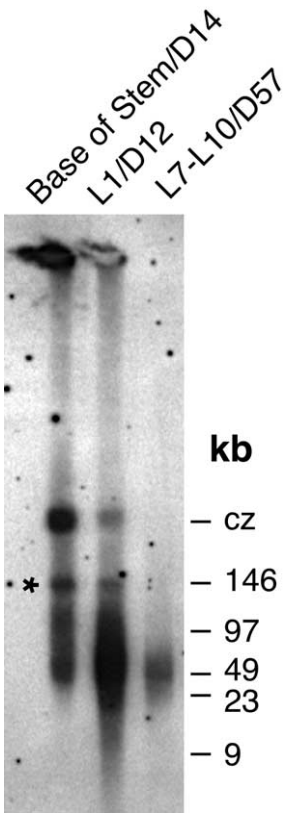

Figure 10. Blot-hybridization of plastid DNA from juvenile and adult plants. Plastid DNA from juvenile (the base of the stem at day 14 and leaf blade L1 at day 12) and adult (leaf blades L7–L10 at day 57) maize plants was separated by PFGE (10 s pulse time) and hybridized with a plastid-specific *rbc*L gene probe. The volume of plastids used for the DNA in lane Base of stem/D14 was one-third of that for the other two lanes. For equal volumes of plastids, the relative amounts of hybridization throughout each lane (including immobile and mobile fractions) are 12 : 5 : 1 for the three lanes, respectively. An asterisk (*) indicates the linear DNA band at 140 kb (the size of the genome). The compression zone is indicated by cz.

generally decreased as the plastids developed. By stage 5, seven out of 12 fields of class II cpDNA analyzed showed essentially no fibers extending from the cores. On the other hand, the number of unconnected fibers (irrespective of class type) changed greatly during development. The maximum number of unconnected fibers per field illustrated these changes. The numbers were 21 for juvenile plant stems at stage 1, 100 for the juvenile leaf blade at stage 5, and 22 for the adult leaf blade at stage 6. This change in cpDNA structure with leaf or plant age again suggests a conversion from complex, multigenomic, replicating forms to simple forms, as replication ceases and cpDNA molecules disperse throughout the chloroplasts. Finally, the cpDNA is degraded after the chloroplasts have fully matured.

Discussion

Most studies of the chloroplast and its DNA are conducted at either of two levels of resolution. One level includes plastid development, nucleoid morphology, and DNA content per plastid, and the other focuses on molecular structure, replication, and genome organization. Entire shoots from a single stage of development is the typical source for cpDNA, as in our previous study, where we found several structural forms of maize cpDNA in young seedlings.[4] In this study, we conducted an analysis of plastid development at both levels of resolution. We used juvenile and adult plants to determine whether the form of the DNA changes during replication and segregation of the chloroplast chromosome. We employed three methods of analysis: DAPI-DNA fluorescence of chloroplasts, single-molecule imaging, and PFGE/blot-hybridization. Our results show that cpDNA changes from branched multigenomic forms to simple linear forms during plastid development (circular forms are rare). These changes in molecular structure are accompanied by massive changes in plastid DNA content. Our results indicate that the chloroplast chromosome exists as a multigenomic structure of variable size, rather than the genome-sized circular form depicted in the conventional view of cpDNA. Most surprising is our finding that during chloroplast maturation the size of cpDNA molecules decreases progressively to less-than-genome-sized fragments until no cpDNA is detectable in most of the chloroplasts from leaf blades of juvenile and adult plants.

What is the smallest amount of cpDNA we could detect? Visual inspection readily revealed a spot of DAPI fluorescence from individual P22 phage particles, which contain a 42 kb genome. Since we found no fluorescent spots in most of the chloroplasts from mature leaves, our detection limit might be 42 kb if all that DNA was present in a single nucleoid. In our quantitative fluorescence assay, one pixel·μm^2 represents 9 kb of DNA. Since 14 pixel·μm^2 (representing 0.9 chloroplast genome equivalent or 126 kb of DNA) was the lowest level of DAPI fluorescence we found among 185 DNA-containing chloroplasts, the chloroplasts exhibiting no DAPI fluorescence (the "no-DNA" chloroplasts) might contain less than 9 kb of DNA. Regardless of the uncertainty of our lower limit of detection, an amount of DNA less than 140 kb does not represent an intact genome, has no genetic significance and, at best, might produce some transcripts before the degradation of cpDNA progresses to completion.

Leaf and chloroplast development

The maize leaf can be divided into three distinct regions: the sheath, the ligule, and the blade. Development progresses from undifferentiated tissue at the base of the sheath or stem to differentiated tissue at the tip of the blade.[24,28] Sylvester *et al.*[24] described three stages of leaf

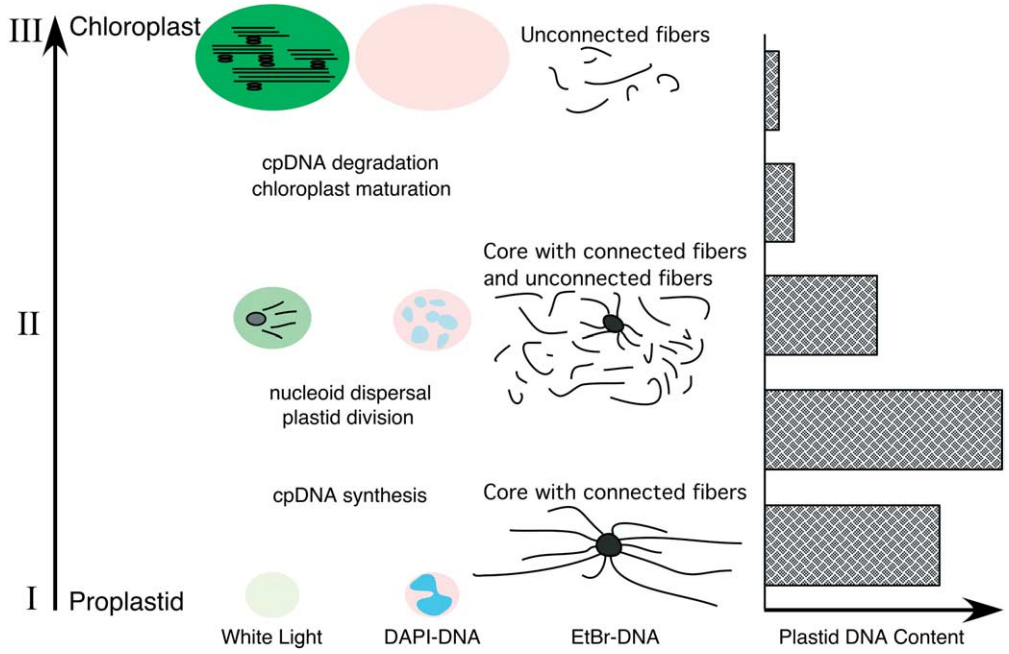

Figure 11. Stages of chloroplast development. The progression of chloroplast development can be divided into three stages (I–III). For each stage, the appearance of the plastids (white light), nucleoids (DAPI-DNA), and cpDNA (EtBr-DNA) is illustrated. The relative change in DNA content per plastid during development is also shown. Each stage is described in the text.

growth: the preligule stage with undifferentiated and dividing cells, the blade growth stage with some division continuing in the sheath and differentiation in the blade, and the sheath growth stage with differentiation in the sheath. Growth of the cell may be divided into three stages: cell division, cell expansion or elongation, and cell differentiation. Similarly, the progression of plastid development may be separated into three stages (Figure 11). Stage I represents undifferentiated proplastids in cells at or near the meristematic region. Stage II includes dividing and developing plastids in dividing and expanding cells. Stage III consists of the mature, green chloroplasts in differentiated leaf cells. We now integrate information about leaf and plastid development with cpDNA structure, replication and inheritance.

Stage I: cell division, plastid division, and plastid DNA replication

The meristematic tissue is localized primarily at the leaf base, although some cell division occurs throughout the length of the developing sheath,[24] and transcription is low in proplastids.[29] We found mostly small, colorless, undeveloped proplastids at the base of the stem in juvenile plants. There was relatively high DAPI-DNA fluorescence in the proplastids, typically with only one or two nucleoids per plastid that appeared as continuous fluorescent strands throughout the plastids. The genome copy number varied among the proplastids, and in the youngest tissue we found at least 24 copies (genome equivalents) per plastid. The multigenomic complexes in proplastids result from DNA replication, as described below. Plastid DNA replication has been shown to be high in meristematic tissue from barley,[15] oat,[13] wheat[14,30] and *Arabidopsis*.[31]

Stage II: cell expansion, plastid division, and nucleoid partitioning

In the stem above the basal meristem, the cells are engaged primarily in cell expansion, although there is some cell division.[24] The number of plastids per cell increases through plastid division, and plastids are beginning to differentiate into chloroplasts or other plastid types.[3,32] Photosynthetic gene transcription and mRNA copy number are high at this stage of chloroplast differentiation.[29] We find that plastids from the stem tissue are variable in appearance, larger than at stage I, beginning to green, and show morphological features that may represent prolamellar bodies. Most plastids have intense DAPI-DNA fluorescence (suggesting continued cpDNA replication), and the several discrete nucleoids (five to ten per plastid) we find are probably en route to daughter plastids during division. We suggest that at this stage cpDNA replication proceeds primarily through an origin-independent, recombination-dependent process, as described below. The cpDNA is found mostly in complex structures that contain many genome copies, but complexes are beginning to be processed to smaller branched structures and simpler linear forms as forks reach the ends of template strands.

Stage III: cell differentiation, chloroplast maturation, and cpDNA degradation

Cell division and growth have ceased, transcription of cpDNA has decreased,[29] and plastids have fully differentiated into mature chloroplasts. The final events in leaf development involve differentiation to specific cell and plastid types. There are two maize cell types that contain mature chloroplasts: mesophyll (MS) and bundle sheath (BS) cells. Lindbeck *et al*.[33] reported differences in chloroplast morphology and nucleoid size and number, but similar DNA content per plastid for these two cell types. Although discrete DAPI-DNA nucleoids were observed in the chloroplasts from both cell types, no information was provided as to whether all or only some of the chloroplasts had DAPI-DNA nucleoids. The chloroplasts were relatively small (average size 13–15 μm^2) in the cells from young seedlings. In contrast, we did not distinguish between chloroplasts from different cell types and the chloroplasts, with a few exceptions, were large ($>20\ \mu m^2$), green, and uniform in appearance for both juvenile and adult leaves. Furthermore, DAPI-DNA fluorescence was undetectable in 53–89% of the chloroplasts. We suspect that the small chloroplasts with DAPI-DNA nucleoids from the MS and BS cells described by Lindbeck *et al*.[33] were closer developmentally to those at stage II than mature chloroplasts at stage III. We suggest that at stage III cpDNA replication has ceased, and the complex branched forms are processed progressively to simple individual molecules with increasing leaf age. Ultimately, the cpDNA is degraded to undetectable levels in the mature chloroplasts, apparently because DNA is no longer needed in adult leaves engaged in photosynthesis (see below).

To summarize, at stage I both cells and plastids divide, and plastids show high DNA replication activity, high genome copy number per plastid, and low plastid transcriptional activity. The cpDNA exists primarily as branched multigenomic complexes with a few simple molecules. At stage II, cpDNA replication is winding down, but genome copy number per plastid is high, as are plastid transcriptional and translational activities, and cell expansion is accompanied by plastid division. The nucleoids disperse throughout the expanding chloroplasts, and are partitioned to daughter chloroplasts as progressively smaller and simpler chromosomal DNA molecules. At stage III, cell and plastid development is complete, and cpDNA is degraded first to subgenomic fragments and then entirely.

Origin paired linear isomers recombination-dependent replication model for cpDNA

The standard model for cpDNA replication involves a genome-sized circular molecule and D-loop-to-theta-to-rolling circle replication to produce more genome-sized circles.[2,34,35] In addition, cpDNA is generally assumed to exist as two circular isomers with an inversion of the long single copy (LSC) region produced by recombination between large inverted repeat (IR) sequences, a process termed "flipping".[36,37] We recently proposed an alternative model involving only linear molecules and a recombination-dependent replication (RDR) mechanism.[4,38] That model began with a genomic monomer invading a homologous region of a concatemer and showed how isomeric forms with an inverted LSC and branched multigenomic structure could be generated. We now expand on the model, which we term the Origin Paired Linear Isomers RDR (OPaLI-RDR) mechanism, to show how replication is initiated, as well as the formation of head-to-tail (h-t) concatemers.

We previously described similarities between maize cpDNA and herpes simplex virus (HSV) DNA, including linear genome-sized molecules with defined ends, isomers with inverted single-copy regions,[4] and a recent revision of the assumption that replication involved a circular intermediate.[39] We now describe features that cpDNA and HSV DNA share with the DNA from bacteriophage T7 DNA, including head-to-tail (h-t) linear concatemers and branched multigenomic complexes. T7 DNA has direct repeat sequences at the ends of each monomer unit, so that the DNA molecules are terminally redundant and can form h-t concatemers by recombination between identical molecules (Figure 12(a)).[40] For HSV DNA, there is a region of direct repeats within the IRs that also creates a terminal redundancy and the possibility of forming h-t concatemers.[40,41] The cpDNA of maize is not terminally redundant, but the isomers share one set of direct repeat sequences at one end (the left end of one isomer and right end of the other) and completely different sequences at the other ends (Figure 12(a) and (b)). Recombination between isomers can therefore lead to h-t linear concatemers.

Another similarity between T7 DNA and cpDNA is the location of the origin(s) of replication near, but not at, the ends of the linear molecules. Whereas T7 has only one origin, maize cpDNA has two putative origins (*ori*A and *ori*B) within the terminal IR,[4] near the right end of one isomer and near the left end of the other (Figure 12(b)). (Note that both isomers have a second set of origins in the internal IRs.) Figure 12(c) shows a T7-like model for cpDNA replication that can lead to an h-t concatemer. Replication begins at a different origin on each isomer (step 1), resulting in daughter molecules with incompletely replicated 3′ ends (step 2). Compatible single-strand regions are produced when replication is initiated at *ori*A on the right end of one isomer and at *ori*B on the left end of the other isomer (double-headed arrow in step 3), and these anneal (step 4). The excess 3′ overhang is then removed to produce an h-t concatemer (step 5). Since only the sequence between the two origins can provide compatible single-strand regions, an h-t concatemer will not result from initiation at either the same origin on both isomers or at *ori*B on the left isomer and *ori*A on the right isomer. For T7

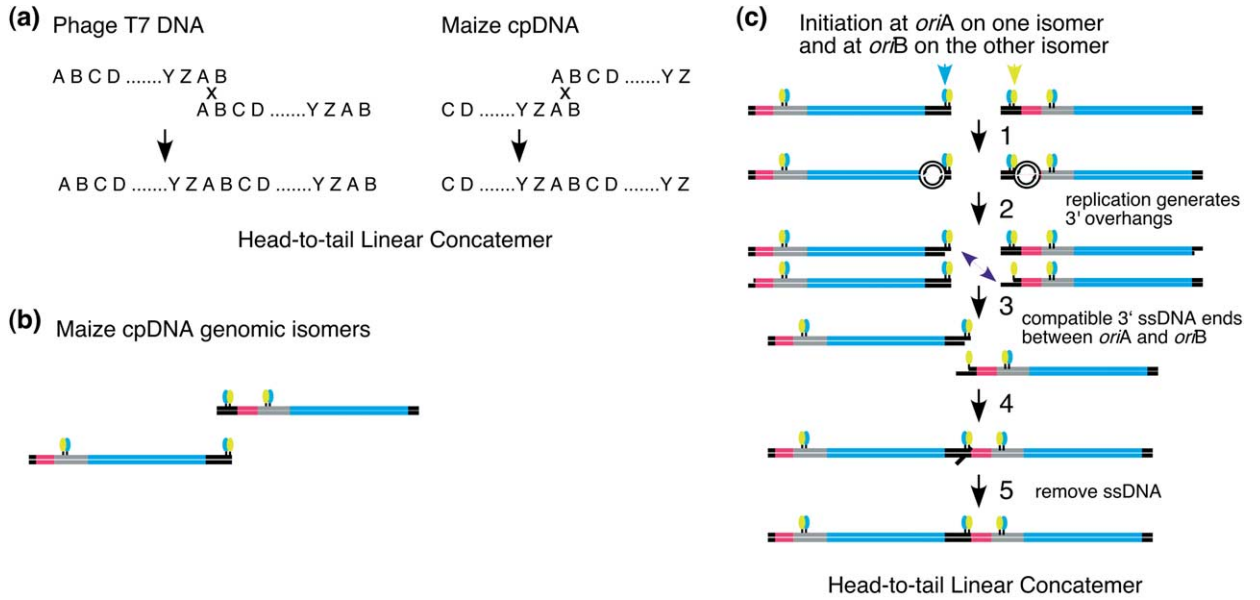

Figure 12. Origin paired linear isomers (OPaLI): A model for chloroplast DNA replication initiation and concatemer formation. (a) Formation of a head-to-tail (h-t) concatemer. For phage T7, all genome-sized molecules are identical and have the same direct repeat sequence (AB) at both ends (terminal redundancy).[40] For maize cpDNA, a pair of genome-sized isomers have the same sequence (AB) at one end, but different sequences at the other ends (YZ and CD). (b) Maps of maize cpDNA showing linear genome-sized isomers with different ends.[4] The isomers have one common end sequence containing two putative replication origins indicated by the blue oval (homolog of *Oenothera ori*A) and the yellow oval (homolog of *Oenothera ori*B).[4] The long single-copy region is shown in blue, the short single-copy region is red, and the inverted repeats (IR_A and IR_B) are indicated by the grey and black lines, respectively. (c) Initiation of replication at different origins on each isomer produces an h-t concatemer because the nascent molecules have compatible 3′ overhangs in the region between *ori*A and *ori*B. Step 1: bidirectional replication is initiated at *ori*A on one isomer (short blue arrow) and at *ori*B on the other isomer (short yellow arrow), producing bubbles (the lagging strand is shown as continuous for simplicity). Step 2: four new molecules are produced, each with one blunt end and one 3′ overhang. Step 3: two nascent molecules (indicated by the double-headed arrow) are aligned by pairing the origins to show that their single-strand 3′ ends are compatible. (Note that an h-t concatemer would not be produced from initiation at the same origin, either *ori*A or *ori*B, on both isomers because the nascent molecules would have non-compatible 3′ overhangs.) Step 4: the two nascent molecules are annealed at the compatible sequences, but a single-strand region protrudes. Step 5: an h-t concatemer is formed after removal of the protrusion and sealing of gaps by ligation. This model can apply to chloroplast genomes without IR sequences, such as in pea[57] and *Medicago truncatula*(Genbank accession no. AC093544).

DNA, initiation at a single origin creates the compatible 3′ overhangs because all molecules are identical with the same left and right ends. Thus, for an analogous replication mechanism, only one origin per genome is needed to create a T7 concatemer starting with identical units, whereas two origins are required for cpDNA comprised of non-identical units. The presence of closely spaced origins might, in fact, indicate that OPaLI-RDR is used to replicate the cpDNAs of any plant, irrespective of whether it contains the IR found in most species.

The production of the h-t concatemers of cpDNA still leaves two potential problems: the concatemer is not a true dimer, since duplication of part of the junction region would be required to produce two complete monomer units; and two of the four newly replicated molecules do not have compatible 3′ overhangs and still need terminal sequences filled in. The first problem may be solved as proposed for the resolution/maturation of T7 DNA: nicking and/or double-strand breaks and strand displacement accompanied by replication.[40] To solve the second problem, the single-strand 3′ overhang can invade a homologous region of another molecule, either a monomer or a concatemer (step 1 in Figure 13). Additional strand invasion and RDR, as proposed for T7, would then create the branched multigenomic molecules that are the major form of cpDNA found in the undeveloped plastids (step 2). Strand invasion of the h-t concatemer may also avoid the problem created by this concatemer being an incomplete dimer.

One of the characteristics of both nucleoids within chloroplasts and the EtBr-DNA stained molecules we find for maize and *Arabidopsis*[23] is variability in size and appearance. The completion of replication at different forks and/or recombination may result in molecules of various size and structure: circular and linear monomers, multigenomic h-t concatemers and sub-genomic pieces, and smaller branched complexes (step 3 in Figure 13). The circular forms may merely be by-products of recombination, as we suggested for mitochondrial DNA (mtDNA) from liverwort.[42] Forks reaching the ends of template strands without

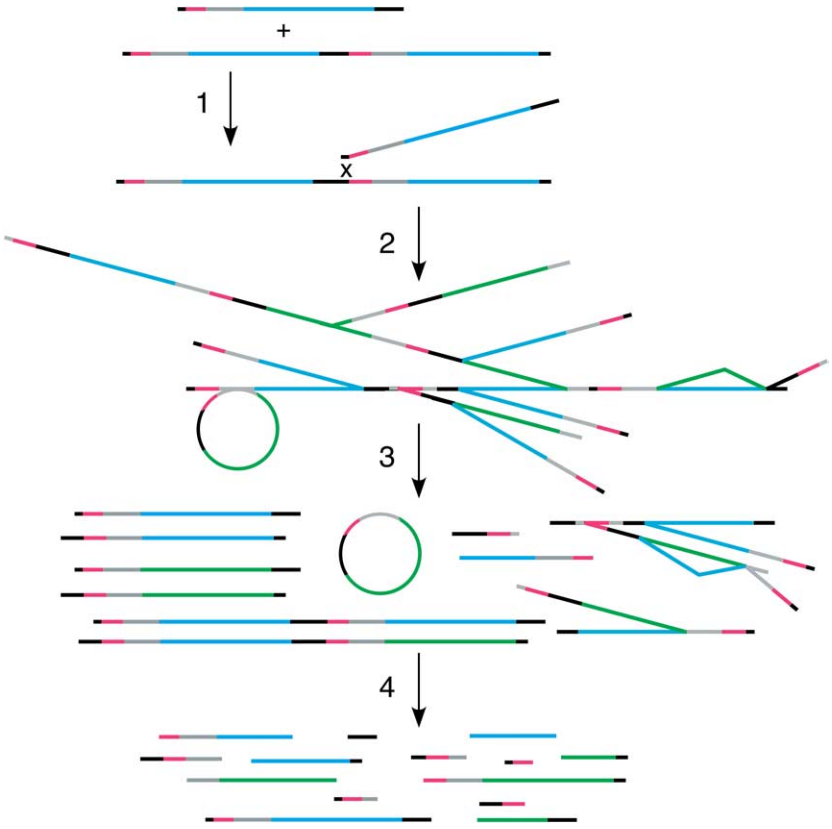

Figure 13. From multigenomic to subgenomic forms: recombination-dependent replication and degradation of chloroplast DNA. Step 1: the products of the OPaLI mechanism shown in Figure 12(c) are genome-sized linears with single-strand 3′ overhangs and an h-t dimer. The single-strand end of the monomer invades the homologous region of the dimer to initiate replication. The long single-copy region (LSC) is shown in blue, the short single-copy region is red, and the inverted repeats (IR_A and IR_B) are indicated by the grey and black lines, respectively. Step 2: continued strand invasion and replication generates a branched structure containing many genome equivalents of cpDNA. A blue or green (inverted) LSC orientation depends on whether strand invasion occurs at IR_A or IR_B.[4] Step 3: replication ceases, and smaller forms arise as forks reach the ends of their template strands and branchpoints are resolved by recombination. The four linear monomers (two with blue and two with green LSCs) and two h-t dimers that are shown (on the left) were predicted by restriction mapping.[4] Incidental recombination of direct repeat sequences (IR_A in this example) on an h-t concatemer produces a genome-sized circle. Step 4: degradation leaves most of the cpDNA as less-than-genome-sized fragments (a genome-sized molecule is shown at bottom left), perhaps by metallo-nucleases as suggested for rice cpDNA.[22] Continued degradation eliminates the DNA from most mature chloroplasts (Figure 5).

reinitiation of replication and degradation of cpDNA would result in further breakdown to molecules of variable size, including the less-than-genome-size molecules (step 4) that appear as smears in PFGE (see Figure 10 and Refs 4, 43 and 44).

The OPaLI-RDR model accounts for the two closely spaced origins and two cpDNA isomers previously identified, and it applies to cpDNAs with and without IRs. Finally, it accounts for the myriad of structural forms observed including circular, linear, and branched multigenomic complexes.

Photosynthesis without chloroplast DNA

One might expect to find substantial amounts of DNA in mature chloroplasts for several reasons. Numerous photosynthesis genes are located on cpDNA, and some of their products turn over rapidly.[45–47] Green leaves have been the most common tissue from which cpDNA is obtained,[43,48–50] and hundreds of genome equivalents per chloroplast are commonly reported.[51] Chromosomal DNA molecules are usually considered to be quite stable, although this generality is based largely on studies of nuclear DNA. On the other hand, chloroplast ploidy levels are typically expressed as average values for young seedlings and not mature leaves,[11,13–15] and the stability exhibited for nuclear DNA may not apply to cpDNA. As we show here with maize, and previously with *Arabidopsis*,[23] mature chloroplasts with no detectable DNA can persist in green leaves. DNA could be dispensable in mature chloroplasts if either the photosynthetic proteins or mRNAs were stable.

Most photosystem proteins encoded by the chloroplast genome are stable, and their mRNAs turn over rapidly.[29,47] On the other hand, the D1 protein (the *psb*A gene product) in the photosystem II reaction center is prone to damage and must be replaced continually. The *psb*A mRNA is stable in mature chloroplasts and, in fact, its stability increases during chloroplast maturation.[52] Furthermore, after docking of the *psb*A mRNA–ribosome–nascent D1 protein complex at the thylakoid membrane, translation is arrested and does not proceed until new D1 protein is needed to replace the damaged protein.[47,53] Thus, the retention of cpDNA would not be required for continued photosynthetic activity if the required proteins were stable or could be produced from stable mRNAs.

Is the degradation of the cpDNA beneficial for the plant? The degradation of cpDNA and mtDNA was previously shown to occur under certain conditions, including just before leaf senescence in rice,[21,22] and as the basis for uniparental

inheritance.[19,20,54] The degradation of cpDNA is not likely to trigger leaf senescence in maize because we find that adult leaves without cpDNA persist for three months before showing any sign of yellowing. The degradation of cpDNA in *Chlamydomonas* was proposed as a response to nutrient starvation that inadvertently leads to uniparental inheritance.[20] The most instructive example of organellar DNA turnover is found during the maturation of (non-photosynthetic) pollen in angiosperms.[54] Whereas the elimination of cpDNA and/or mtDNA from the generative cell of the pollen grain correlates perfectly with the uni- or biparental mode of organellar inheritance, both cpDNA and mtDNA are always degraded during development of the vegetative cell (which does not contribute to the zygote) of the pollen grain regardless of the organellar inheritance pattern. Thus, the demise of organellar DNA can be independent of its effect on either leaf senescence or the mode of organellar inheritance.

We suggest that the degradation of cpDNA during maize chloroplast maturation can benefit the plant in two ways. Nucleotides may be recycled for their nutritive value, and the elimination of cpDNA relieves the cell of the burden of maintaining and repairing the many copies of the chloroplast genome that are no longer needed for their coding function.

Materials and Methods

Preparation of chloroplasts and cpDNA

Maize juvenile seedlings (*Zea mays* L. cv. Mycogen 2722-1M1) were grown for eight to 16 days in vermiculite on 16 hours light/eight hours dark cycles at 23–25 °C. For adult plants, individual seedlings were transplanted into six-inch pots with soil and grown in the greenhouse. Entire juvenile seedlings (including the seed but with roots removed) or adult leaf blades were harvested and washed for one to three minutes in 0.5% (v/v) Sarkosyl, then rinsed exhaustively in water (in order to minimize microbial contamination). For seedlings, the coleoptile was removed, and 0.5 cm tissue sections were excised from the stem and leaves as shown in Figure 1. For adult leaves, either a 1 cm segment from the center of the blade or the entire leaf blade was used after the midrib of the blade was removed. Tissue was homogenized in grinding buffer (0.33 M sorbitol, 50 mM Hepes (pH 7.6), 1 mM $MgCl_2$, 2 mM EDTA, 0.1% (w/v) bovine serum albumin (BSA), 1% (w/v) polyvinylpyrrolidine-40) using either a mortar and pestle or a Waring blender.[4] The homogenate was filtered through one to three layers of Miracloth, centrifuged, and the plastids washed with dilution buffer (0.33 M sorbitol, 20 mM Hepes (pH 7.6), 1 mM $MgCl_2$, 2 mM EDTA, 0.1% BSA), treated with DNase, and purified on 30/70% (w/v) Percoll gradients.[4,23]

For fluorescence microscopic imaging of the DAPI-stained plastids, the plastids were fixed in 0.4–0.8% (v/v) gluteraldehyde and stored at 4 °C, stained with 1–2 μg/ml of DAPI, and 1% (v/v) β-mercaptoethanol (βME) was added to reduce fading.[6,55] Particles of vaccinia virus[26] and bacteriophages T4 (ATCC 11303-B4) and P22 (provided by Kelly Hughes) were stained and imaged by the procedures used for plastids. Chloroplasts from adult plants (L7/D65) were prepared with and without DNase before fixation in gluteraldehyde and staining with DAPI to assess whether mature chloroplasts were permeable to DNase. Imaging was performed also with fixed plastids but without the addition of DAPI. For treatment with DNase, the fixed plastids were washed twice with TE (10 mM Tris (pH 8), 1 mM EDTA), resuspended in dilution buffer plus 10 mM $MgCl_2$, and incubated with 300 μg/ml of DNase overnight at 4 °C prior to imaging with DAPI and βME. Imaging without DAPI and after DNase-with-DAPI yielded similar results; a reddish tinge (weak plastid autofluorescence) but no blue-white DAPI-DNA fluorescence was observed in plastids from both juvenile and adult tissues.

For PFGE and fluorescence microscopic imaging of the cpDNA, the plastids were embedded in agarose and lysed overnight at 48 °C in 40 mM EDTA (pH 8), 1% Sarkosyl with 200 μg/ml of proteinase K.[4] Phenylmethylsulfonyl fluoride (PMSF) was used to inactivate proteinase K, and samples were washed extensively in TE and stored at 4 °C in TE. PFGE and blot hybridization to a *rbc*L gene probe was performed[4] using cpDNA isolated from the base of the stem of 14 days old juvenile seedlings, L2 of 12 days old juvenile seedlings, and L7–L10 of 57 days old adult plants. A digitized image of the hybridization signal and NIH ImageJ were used to estimate the amount of DNA in each lane.[4]

White light microscopy and fluorescence microscopy of chloroplasts

For each field of plastids (±DAPI and ±DNase), multiple images were acquired using white light (no filter) and a DAPI filter (D360ext/460emt), a Nikon Microphot-FX epi-fluorescence microscope equipped with a QImaging Retiga 1300 digital camera using Open*lab*™ image capture and analysis software. A single field of view was equivalent to an area 90 μm×70 μm on a microscope slide at the highest resolution (1024×768 pixels) of the digital camera and displayed on a computer screen. An image of an objective micrometer was used to calibrate the field of view. Using Open*lab*™, the plastid area (μm^2) and DAPI fluorescence intensity (FI; grayscale pixel values from 0 to 1023) were measured. For quantitification of the CorTotal DAPI F/plastid (as given in Table 1), two corrections were necessary: one to account for the variation of the background FI between fields and the other to account for plastid autofluorescence.

For the first correction, the average background FI for all of the DAPI images was determined. This is the "standard background FI" (std bg FI) and was used to adjust the DAPI FI/plastid (Table 1) from the measured DAPI FI of the plastid and the measured background FI (bg FI) of the field. For example, the measured DAPI FI (mFI) for a plastid was 463 pixels, the field bg FI was 50 pixels, and the std bg FI (used for all fields) was 75 pixels. The DAPI FI/plastid was then calculated as 620 pixels using the equation: DAPI FI/plastid = (DAPI mFI [std bg FI/bg FI]) − std bg FI. The total DAPI F/plastid (2914 pixel·μm^2 in the example) was determined by multiplying the DAPI FI/plastid (620 pixels) by the plastid area (4.7 μm^2; determined from the DAPI image).

For the plastid autofluorescence correction, the DAPI AFI (autofluorescence intensity) and total DAPI AF (autofluorescence) per plastid were determined for the plastids prepared without-DAPI and after DNase-with-DAPI. A linear correlation was obtained by plotting

plastid area (x-axis; determined from white light image) *versus* total DAPI AF/plastid (y-axis). The equation from this plot, $y = -578.35 + 117.42x$, $R = 0.888$, was used to calculate the amount of total DAPI F/plastid that was attributed to plastid autofluorescence which was then subtracted to give the CorTotal DAPI F/plastid. Continuing the example above, the CorTotal DAPI F/plastid is 2811 pixel·μm^2, obtained by subtracting 103 pixel·μm^2 (the amount of autofluorescence) from 2914 pixel·μm^2 (the total DAPI F/plastid). The plastid area determined from the white light image was 5.8 μm^2. This is an example of a proplastid from the base of stem with very little autofluorescence. For mature chloroplasts most, if not all, of the measured total DAPI F/plastid is due to autofluorescence. For example, in one chloroplast from the first juvenile leaf the total DAPI F was 4076 pixel·μm^2 and the CorTotal F was 588 pixel·μm^2; thus 3488 pixel·μm^2 was due to autofluorescence, and in one chloroplast from the adult leaf the entire total DAPI F/plastid of 4830 pixel·μm^2 was attributed to autofluorescence.

The genome copy number per maize plastid was determined using a method analogous to that described by Miyamura *et al*.[8] and relative to both vaccinia virus and bacteriophage T4 DNAs. The DAPI-DNA fluorescence intensity and area were measured for 151 virus particles and 150 phage particles using the same system as described above for the plastids. The DAPI FI was 122($\pm$32) pixels for vaccinia and 49($\pm$15) pixels for T4 particles, and the areas were 0.20($\pm$0.07) μm^2 and 0.20($\pm$0.08) μm^2, respectively. The total DAPI F/virus or phage particle was determined as 25($\pm$11) pixel·μm^2 and 10($\pm$6) pixel·μm^2, respectively. This value was used to calculate the relative fluorescence intensity of plastid to vaccinia particle, the vaccinia virus equivalents or V units (V = CorTotal DAPI F/plastid divided by average total DAPI F/particle). Using vaccinia as the standard, the genome copy number was then calculated using the equation: copy number = 1.52 V. The value 1.52 is a constant factor that accounts for the difference in DNA base composition and size between the vaccinia virus and maize plastid genomes and was determined as (%(A + T) of virus genome/%(A + T) of plastid genome) × (bp vaccinia DNA/bp maize cpDNA), where %(A + T) for vaccinia (Copenhagen strain) is 66.6, %(A + T) for maize is 61.5, bp for vaccinia (strain vTF7.3) is 197,361, and bp for maize is 140,387. Again, using the proplastid example above, the copy number is 171, using 1.52 V, where V = 2811 pixel·μm^2 plastid/25 pixel·μm^2 virus. The theoretical detection limit is 1 pixel·μm^2 and corresponds to ~9 kb based on: 1 pixel·μm^2 CorTotal DAPI F per plastid/25 pixel·μm^2 per virus particle = 0.04 V unit; 0.04 V unit × 1.52 = 0.06 plastid genome equivalents; 0.06 genome equivalents × 140 kb per genome = 8.5 kb. A plastid with a genome copy number equal to one would have a CorTotal DAPI F of 16($\pm$8) pixel·μm^2 and is equivalent to 0.64($\pm$0.32) V units (the copy number per plastid was rounded to the nearest whole number). The copy number relative to T4 was determined by a similar manner but using 65.5%(A + T) and 168,903 bp.

Fluorescence microscopy of cpDNA

Ethidium bromide-stained cpDNA (0.1 μg/ml of EtBr) images were produced using a G-1B filter (546ext/DM580/590emt) with the system described above and elsewhere.[4,42,56] Chloroplasts were suspended in agarose at dilutions that showed all the DNA from a single chloroplast within a single field of view.[4] Typically, a 200 to 1000-fold dilution (of that used to produce EtBr-stained images in PFGE) was used, which still provided a sufficient concentration of EtBr-DNA molecules per slide for convenient visual analysis. The paucity of cpDNA in the adult leaf blade is illustrated by the difficulty in finding any EtBr-DNA molecules at all. For example, EtBr-DNA images from the base of a young seedling (D9) were made using a 1 : 1000 dilution with DNA molecules present in almost every field of view on a single slide. On the other hand, for the adult leaf tissue (L7–L10/D57) at a 1 : 200 dilution, only five fields with multiple fibers and an occasional field with a single molecule were found on an entire microscope slide.

The images in Figures 8 and 9 are shown in an inverted (white background with black DNA) format. The EtBr-DNA fluorescence images were recorded originally as black background with white DNA. The brightness and contrast of the images have been adjusted to enhance visualization of individual fibers and simple molecules, generally resulting in overexposure of the fluorescence within the core of the complex structures.

Acknowledgements

This research was supported by the United States Department of Agriculture (grant no. 2002-35301-12021). Maize seed was provided by Arthur H. Oldenburg. We thank Doug Ewing for assistance with growing maize.

References

1. Kolodner, R. & Tewari, K. K. (1972). Molecular size and conformation of chloroplast deoxyribonucleic acid from pea leaves. *J. Biol. Chem.* **247**, 6355–6364.
2. Kolodner, R. D. & Tewari, K. K. (1975). Chloroplast DNA from higher plants replicates by both the Cairns and the rolling circle mechanism. *Nature*, **256**, 708–711.
3. Kuroiwa, T. (1991). The replication, differentiation, and inheritance of plastids with emphasis on the concept of organelle nuclei. *Int. Rev. Cytol.* **128**, 1–62.
4. Oldenburg, D. J. & Bendich, A. J. (2004). Most chloroplast DNA of maize seedlings in linear molecules with defined ends and branched forms. *J. Mol. Biol.* **335**, 953–970.
5. Coleman, A. W. (1979). Use of the fluorochrome 4′6-diamidino-2-phenylindole in genetic and developmental studies of chloroplast DNA. *J. Cell Biol.* **82**, 299–305.
6. Kuroiwa, T., Suzuki, T., Ogawa, K. & Kawano, S. (1981). The chloroplast nucleus: distribution, number, size, and shape, and a model for multiplication of the chloroplast genome during chloroplast development. *Plant Cell Physiol.* **22**, 381–396.
7. Lawrence, M. E. & Possingham, J. V. (1986). Direct measurement of femtogram amounts of DNA in cells and chloroplasts by quantitative microspectrofluorometry. *J. Histochem. Cytochem.* **34**, 761–768.
8. Miyamura, S., Nagata, T. & Kuroiwa, T. (1986). Quantitative fluorescence microscopy on dynamic changes of plastid nucleoids during wheat development. *Protoplasma*, **133**, 66–72.

9. Scott, N. S. & Possingham, J. V. (1980). Chloroplast DNA in expanding spinach leaves. *J. Expt. Bot.* **31**, 1081–1092.
10. Lamppa, G. K., Elliot, L. V. & Bendich, A. J. (1980). Changes in chloroplast number during pea leaf development: an analysis of a protoplast population. *Planta*, **148**, 437–443.
11. Dubell, A. N. & Mullet, J. E. (1995). Continuous far-red light activates plastid DNA synthesis in pea leaves but not full cell enlargement or an increase in plastid number per cell. *Plant Physiol.* **109**, 95–103.
12. Hashimoto, H. (1985). Changes in distribution of nucleoids in developing and dividing chloroplasts and etioplasts of *Avena sativa*. *Protoplasma*, **127**, 119–127.
13. Hashimoto, H. (1989). DNA levels in dividing and developing plastids in expanding primary leaves of *Avena sativa*. *J. Expt. Bot.* **40**, 257–262.
14. Miyamura, S., Kuroiwa, T. & Nagata, T. (1990). Multiplication and differentiation of plastids during development of chloroplasts and etioplasts from proplastids in *Triticum aestivum*. *Plant Cell Physiol.* **31**, 597–602.
15. Baumgartner, B. J., Rapp, J. C. & Mullet, J. E. (1989). Plastid transcription activity and DNA copy number increase early in barley chloroplast development. *Plant Physiol.* **89**, 1011–1018.
16. Woodcock, C. L. F. & Bogorad, L. (1970). Evidence for variation in the quantity of DNA among plastids of *Acetabularia*. *J. Cell Biol.* **44**, 362–375.
17. Lüttke, A. & Bonotto, S. (1981). Chloroplast DNA of *Acetabularia mediterranea*: cell cycle related changes in distribution. *Planta*, **153**, 536–542.
18. Kuroiwa, T., Nishibayashi, S. & Sato, C. (1982). Epifluorescent microscopic evidence for maternal inheritance of chloroplast DNA. *Nature*, **298**, 481–483.
19. Nagata, N., Sodmergen, Sato, C., Sakai, A., Kuroiwa, H. & Kuroiwa, T. (1997). Preferential degradation of plastid DNA with preservation of mitochondrial DNA in the sperm cells of *Pelargonium zonale* during pollen development. *Protoplasma*, **197**, 219–229.
20. Sears, B. B. & VanWinkle-Swift, K. (1994). The salvage—turnover—repair (STOR) model for uniparental inheritance in *Chlamydomonas*: DNA as a source of sustenance. *J. Heredity*, **85**, 366–376.
21. Sodmergen, Kawano, S., Tano, S. & Kuroiwa, T. (1989). Preferential digestion of chloroplast nuclei (nucleoids) during senescence of the coleoptile of *Oryza sativa*. *Protoplasma*, **152**, 65–68.
22. Sodmergen, Kawano, S., Tano, S. & Kuroiwa, T. (1991). Degradation of chloroplast DNA in second leaves of rice (*Oryza sativa*) before leaf yellowing. *Protoplasma*, **160**, 89–98.
23. Rowan, B. A., Oldenburg, D. J. & Bendich, A. J. (2004). The demise of chloroplast DNA in *Arabidopsis*. *Curr. Genet.* **46**, 176–181.
24. Sylvester, A. W., Cande, W. Z. & Freeling, M. (1990). Division and differentiation during normal and liguleless-1 maize leaf development. *Development*, **110**, 985–1000.
25. Sekine, K., Hase, T. & Sato, N. (2002). Reversible DNA compaction by sulfite reductase regulates transcriptional activity of chloroplast nucleoids. *J. Biol. Chem.* **277**, 24399–24404.
26. Oldenburg, D. J. & Bendich, A. J. (2001). Mitochondrial DNA from the liverwort *Marchantia polymorpha*: Circularly permuted linear molecules, head-to-tail concatemers, and a 5′ protein. *J. Mol. Biol.* **310**, 549–562.
27. Pedulla, M. L., Ford, M. E., Karthikeyan, T., Houtz, J. M., Hendrix, R. W., Hatfull, G. F. *et al*. (2003). Corrected sequence of the bacteriophage P22 genome. *J. Bacteriol.* **185**, 1475–1477.
28. Stern, D. B., Hanson, M. R. & Barkan, A. (2004). Genetics and genomics of chloroplast biogenesis: maize as a model system. *Trends Plant Sci.* **9**, 293–301.
29. Mullet, J. E. (1993). Dynamic regulation of chloroplast transcription. *Plant Physiol.* **103**, 309–313.
30. Boffey, S. A., Ellis, J. R., Selldén, G. & Leech, R. M. (1979). Chloroplast division and DNA synthesis in light-grown wheat leaves. *Plant Physiol.* **64**, 502–505.
31. Fujie, M., Kuroiwa, H., Kawano, S., Mutoh, S. & Kuroiwa, T. (1994). Behavior of organelles and their nucleoids in the shoot apical meristem during leaf development in *Arabidopsis thaliana* L. *Planta*, **194**, 395–405.
32. Pyke, K. A. (1999). Plastid division and development. *Plant Cell*, **11**, 549–556.
33. Lindbeck, A. G. C., Rose, R. J., Lawrence, M. E. & Possingham, J. V. (1989). The chloroplast nucleoids of the bundle sheath and mesophyll cells of *Zea mays*. *Physiol. Plantarum*, **75**, 7–12.
34. Heinhorst, S. & Cannon, G. C. (1993). DNA replication in chloroplasts. *J. Cell Sci.* **104**, 1–9.
35. Kunnimalaiyaan, M. & Nielsen, B. L. (1997). Chloroplast DNA replication: mechanism, enzymes and replication origins. *J. Plant Biochem. Biotech.* **6**, 1–7.
36. Palmer, J. D. (1983). Chloroplast DNA exists into two orientations. *Nature*, **301**, 92–93.
37. Palmer, J. D. (1985). Comparative organization of chloroplast genomes. *Annu. Rev. Genet.* **19**, 325–354.
38. Bendich, A. J. (2004). Circular chloroplast chromosomes: the grand illusion. *Plant Cell*, **16**, 1661–1666.
39. Jackson, S. A. & DeLuca, N. A. (2003). Relationship of herpes simplex virus genome configuration to productive and persistent infections. *Proc. Natl Acad. Sci. USA*, **100**, 7871–7876.
40. Kornberg, A. & Baker, T. A. (1992). *DNA Replication*. W.H. Freeman and Company, New York.
41. Lehman, I. R. & Boehmer, P. E. (1999). Replication of herpes simplex virus DNA. *J. Biol. Chem.* **274**, 28059–28062.
42. Oldenburg, D. J. & Bendich, A. J. (1998). The structure of mitochondrial DNA from the liverwort *Marchantia polymorpha*. *J. Mol. Biol.* **276**, 745–758.
43. Bendich, A. J. & Smith, S. B. (1990). Moving pictures and pulsed-field gel electrophoresis show linear DNA molecules from chloroplasts and mitochondria. *Curr. Genet.* **17**, 421–425.
44. Lilly, J. W., Havey, M. J., Jackson, S. A. & Jiang, J. (2001). Cytogenomic analyses reveal the structural plasticity of the chloroplast genome in higher plants. *Plant Cell*, **13**, 245–254.
45. Mattoo, A. K., Pick, U., Hoffman-Falk, H. & Edelman, M. (1981). The rapidly metabolized 32,000-dalton polypeptide of the chloroplast is the "proteinaceous shield" regulating photosystem II electron transport and mediating diuron herbicide sensitivity. *Proc. Natl Acad. Sci. USA*, **78**, 1572–1576.
46. Mattoo, A. K., Marder, J. B. & Edelman, M. (1989). Dynamics of the photosystem II reaction center. *Cell*, **56**, 241–246.
47. Baena-González, E. & Aro, E.-M. (2002). Biogenesis, assembly, and turnover of photosystem II units. *Phil. Trans. Roy. Soc. ser. B*, **357**, 1451–1460.
48. Herrmann, R. G., Bohnert, H.-J., Kowallik, K. V. & Schmitt, J. M. (1975). Size, conformation and purity of

chloroplast DNA of some higher plants. *Biochim. Biophys. Acta*, **378**, 305–317.
49. Kolodner, R., Warner, R. C. & Tewari, K. K. (1975). The presence of covalently linked ribonucleotides in the closed circular deoxyribonucleic acid from higher plants. *J. Biol. Chem.* **250**, 7020–7026.
50. Chiu, W.-L. & Sears, B. B. (1992). Electron microscopic localization of replication origins in *Oenothera* chloroplast DNA. *Mol. Gen. Genet.* **232**, 33–39.
51. Bendich, A. J. (1987). Why do chloroplasts and mitochondria contain so many copies of their genome? *BioEssays*, **6**, 279–282.
52. Kim, M., Christopher, D. A. & Mullet, J. E. (1993). Direct evidence for selective modulation of psbA, rpoA, rbcL, and 16S RNA stability during barley chloroplast development. *Plant Mol. Biol.* **22**, 447–463.
53. Zhang, L., Paakkarinen, V., Wijk, K. J. v. & Aro, E.-M. (1999). Co-translational assembly of the D1 protein into photosystem II. *J. Biol. Chem.* **274**, 16062–16067.
54. Nagata, N., Saito, C., Sakai, A., Kuriowa, H. & Kuroiwa, T. (1999). The selective increase or decrease of organellar DNA in generative cells just after pollen mitosis one controls cytoplasmic inheritance. *Planta*, **209**, 53–65.
55. Kuroiwa, T. & Suzuki, T. (1980). An improved method for the demonstration of the *in situ* chloroplast nuclei in higher plants. *Cell Struct. Funct.* **5**, 195–197.
56. Oldenburg, D. J. & Bendich, A. J. (1996). Size and structure of replicating mitochondrial DNA in cultured tobacco cells. *Plant Cell*, **8**, 447–461.
57. Palmer, J. D. & Thompson, W. F. (1981). Rearrangements in the chloroplast genomes of mung bean and pea. *Proc. Natl Acad. Sci. USA*, **78**, 5533–5537.

Edited by J. Karn

(Received 18 August 2004; received in revised form 30 September 2004; accepted 1 October 2004)